

Ultrafine particle exposure concentrations in a residential area near a commercial airport: a repeated measures study in Copenhagen, Denmark

Scientific report, 2024

Prepared by the Environmental Epidemiology Group,
Section of Environmental Health,
Department of Public Health



KØBENHAVNS
UNIVERSITET



Title:

Ultrafine particle exposure concentrations in a residential area near a commercial airport: a repeated measures study in Copenhagen, Denmark

Authors:

Gonzalo B. Hevia-Ramos

Stéphane Tuffier

Marie L. Bergmann

Jiawei Zhang

Steffen Loft

Zorana J. Andersen

Youn-Hee Lim

Thomas Cole-Hunter

Affiliation:

Section of Environmental Health

Department of Public Health

University of Copenhagen

Date:

December 2024

Cover photo:

Branislav Nenin

Contents

Abbreviations.....	1
1. Summary.....	2
2. Background and study objectives.....	3
2.1. Ultrafine particle concentrations in cities.....	3
2.2. Ultrafine particle concentrations near airports.....	4
2.3. Study objectives.....	5
3. Study methods.....	6
3.1. Study setting.....	6
3.2. Study methods.....	7
3.2.1. Ultrafine particle monitoring.....	7
3.2.2. Meteorological monitoring.....	9
3.2.3. Airport flight information.....	9
3.2.4. Statistical analysis.....	10
4. Results: Temporal patterns of ultrafine particle concentration.....	11
5. Results: Spatial patterns of ultrafine particle concentration.....	21
6. Comparison to other airport and city bicycling studies.....	30
6.1. Airport-related studies.....	30
6.2. City-related studies.....	31
6.2.1. Exposures at different times of day.....	31
6.2.2. Exposures at different locations of city.....	31
7. Potential health impacts of observed UFP concentrations.....	37
7.1. Short-term health effects of air quality near airports.....	37
7.2. Long-term health effects of air quality near airports.....	38
8. Conclusion.....	39
References.....	40
Appendix.....	46

Abbreviations

ANOVA	Analysis of Variance (statistical test evaluating differences between group means)
CO₂	Carbon dioxide
COVID-19	Coronavirus disease 2019
CPC	Condensation particle counter
DiSCmini	Diffusion Size Classifier miniature (handheld particle counter, manufactured by Testo)
DMI	Danish Meteorological Institute
GAM	Generalized additive model
GPS	Global Positioning Satellite
LTO	Landing and Take-off term
µg/m³	micrograms per cubic meter
NO₂	Nitrogen dioxide
OSM	OpenStreetMap (free wiki world map)
PM_{2.5}	Particulate matter of diameter <2.5 µm
PNC	Particle number concentration
pt/cm³	Particles per cubic centimetre
P-trak	Ultrafine particle counter (manufactured by TSI)
SD	Standard deviation
UFP	Ultrafine particles (of diameter <0.1 µm)
WHO	World Health Organization

1. Summary

In this study we aimed to map ultrafine particle (UFP, particles of less than 100 nanometres in aerodynamic diameter) concentrations in a typical residential area in the vicinity of Copenhagen airport. Particle number concentrations (PNC, consisting mostly of UFP) were measured using a portable particle counter, in 44 cycling trips (22 trips in the morning between 8:15-9:00 and 22 trips in the afternoon between 12:00-12:45) on a fixed route of ~8,5 km in average and ~40 minutes duration, between July 18th and August 29th, 2024. The study was conducted in the Amager neighbourhood located [3,75-5,75] km north of Copenhagen Airport in Kastrup. Meteorological data (wind direction and speed, humidity, and temperature) was obtained from the Danish Meteorological Institute.

A Spearman correlation test was used to validate DiSCmini measurements with those from a fixed monitoring station. We used Generalized Additive Models (GAM), adjusted for time trends and meteorological variables, to analyse PNC throughout the fixed route. We conducted a geospatial analysis (a method of analysing data linked to specific geographical positions on the earth's surface) for PNC using GPS and OpenStreetMap data.

Our study found average PNC levels of 7,620 pt/cm³ in the 44 repeats of the cycling route in Amager, Denmark. Notably, a southerly or south-easterly wind direction resulted in the highest overall levels (~12,000 pt/cm³) compared to other wind directions (4,000-7,000 pt/cm³), suggesting an influence from the airport, which is located south-east of the studied area. This aligns with other studies showing that airports are sources of UFP emissions, with elevated UFP concentrations detected up to 18 km from the source.

Independently from meteorological factors, high UFP concentrations were observed on busy road segments with traffic congestion and traffic lights (~12,000 pt/cm³), reflecting the typical pattern of traffic as a source of UFP in urban areas. The lowest UFP concentrations (<7,000 pt/cm³) were observed on streets with low traffic and next to a blue space (beach, Amager Strandpark).

Overall, we observed a gradient of increasing UFP concentrations from north to south. In particular, under southerly wind conditions, there was a slight increase in UFP concentrations along the route, with average levels of approximately 12,000 pt/cm³ in the north and 15,000 pt/cm³ in the south of the route respectively. This suggests that in a neighbourhood near an airport, the diffusion of UFP emissions from such a source is influenced primarily by wind direction and may gradually be affected by the distance from the airport, contributing to higher UFP concentrations.

2. Background and study objectives

2.1. Ultrafine particle concentrations in cities

Exposure to ambient air pollution in the form of particulate matter below 2.5 μm aerodynamic diameter ($\text{PM}_{2.5}$) is known to cause adverse health effects such as cardiovascular and respiratory diseases, contributing to approximately five million deaths worldwide every year (Health Effects Institute, 2024). Recently, there has been increasing research interest in ultrafine particles (UFP), which are the smallest fraction of particulate matter below 0.1 μm , or 100 nm, in aerodynamic diameter. UFP by their small size are also low in mass, and thus not well represented in the routinely monitored particle mass concentration, and typically presented as particle number concentration (PNC). UFP also differ from larger particles in ambient air in terms of their primary sources, which are road traffic emissions in urban areas with some contributions from airplanes emissions, wood stoves, construction work and other combustion processes (Morawska et al., 2019); and, in their short lifespan in the air and large spatial and temporal variation. The health concerns related to UFP are caused by their relatively higher toxicity related to their relatively higher surface area per mass compared to larger particles, and thus greater ability to carry (adsorb) large amounts of potentially toxic co-combustion-emitted materials. Additionally, their smaller size allows them a greater ability to enter deep into the lungs, and if small enough, cross into the blood stream, and translocate to other organs including the brain and nervous system (Ohlwein et al., 2019). So, generally, the smaller the particle, the higher the potential toxicity of that particle. While the World Health Organization (WHO) has no set guideline on UFP, they do have a four good practice statements (WHO, 2021), briefly summarised as:

1. Quantify ambient UFP in terms of PNC for a size range from ≤ 10 nm and greater;
2. Integrate UFP monitoring as size-segregated real-time PNC measurements into existing air quality monitoring programs;
3. Consider $< 1,000$ particles/ cm^3 (24-hr mean) as low and $> 10,000$ particles/ cm^3 (24-hr mean) or $20,000$ particles/ cm^3 (1-hour mean) as high levels of PNC, to guide decision-making on prioritisation of UFP source emission control, and;
4. Use novel science and technology to assess UFP exposure in epidemiological studies and UFP management.

As people move through cities, they encounter peak air pollution concentrations that often far exceed background concentrations. Of particular concern is exposure to UFP, which exhibit large spatial variation; concentrations near a source (such as traffic) can be several times higher than those just a few meters away. As city policies increasingly encourage active mobility such as cycling and walking, it is important to understand the health effects of the increased air pollution exposure in micro-environments close to motorized road traffic exposures. On the one hand, bicycling serves both as regular physical activity to promote individual health and reduces emissions from traffic, improving air quality, to

protect population health. On the other hand, however, bicycling may pose a risk to the cyclist due to the combination of increased breathing rates and immediate proximity to motorized traffic. That is, a cyclist may inhale more polluted air when commuting compared to other commute modes. This then may raise the concern that an increased exposure to air pollution when cycling outweighs the health benefits of the physical activity itself. However, the scientific literature overall indicates that physical activity performance outweighs the health concern from air pollution, assuming that the performer does not have underlying health conditions (Tainio et al., 2016).

Besides road traffic as a source of UFP in urban areas, airports have received increasing attention as emitters of UFP with potential adverse health effects, for airport employees and residents in the vicinity. A global modelling study estimated that aviation emissions are responsible for around 16,000 premature deaths every year worldwide (Yim et al., 2015). Numerous studies document elevated UFP concentrations in and around airports, and an increasing body of literature is available on the health effects of short-term or long-term exposure to airport-related UFP exposure, both in occupational, experimental, or population-based cohort studies (Stacey et al., 2020, Fritz et al., 2022; Gerling and Weber, 2023, Alzahrani et al., 2024).

2.2. Ultrafine particle concentrations near airports

It is well documented that commercial airport activity adversely affects air quality in and around airports. Jet engine emissions from ascending and descending aircraft, the major source of airport-related air pollution, contain large amounts of volatile organic compounds and particulate matter, especially of the smallest particle size fraction in the ultrafine range below 20 nm in diameter (Riley et al., 2021). Pollution emitted from aircraft activities has been found to be equally carcinogenic and with similar adverse health effects as diesel particle emissions (Bendtsen et al., 2021). This causes health concerns for the exposed airport personnel, but also for residents in near airport neighbourhoods. Elevated UFP concentrations have been measured at distances as far as 18 km downwind from airports (Hudda and Fruin, 2016), affecting a potentially large number of people.

A substantial number of studies on fixed-site or mobile UFP measurements in and around commercial airports are available from Europe and the US. Those focusing on residential areas close to airports reported elevated UFP concentrations, such as around major airports in the USA [Boston (Hudda et al., 2020, 2018, 2016), Los Angeles (Choi et al., 2013; Hudda et al., 2014; Hudda and Fruin, 2016; Riley et al., 2016; Shirmohammadi et al., 2017; Westerdahl et al., 2008; Zhu et al., 2011), Roanoke (Klapmeyer and Marr, 2012), Santa Monica (Hu et al., 2009), Warwick (Hsu et al., 2014)], and Europe [Amsterdam (Keuken et al., 2015; Lenssen et al., 2024a; Pirhadi et al., 2020), Berlin (Fritz et al., 2022; Gerling and Weber, 2023), London (Stacey et al., 2020), Madrid (Alzahrani et al., 2024), and Zurich (Zhang et al., 2020)].

Some studies have considered a flight landing and take-off frequency (LTO) term, to capture specific airport-activity-related emission sources (Hsu et al., 2014; Hudda et al., 2018). Hsu and colleagues (2014) found that landings and take-offs on a major runway significantly influenced UFP concentrations in a neighbourhood adjacent to the runway, while Hudda and colleagues (2018) found general aviation-related emissions at a major airport significantly increased UFP concentrations in downwind neighbourhoods. Specifically, UFP concentrations are seen to be elevated under the landing approach path (Riley et al., 2016), and depend on distance to the airport (Chung et al., 2023), wind direction (Keuken et al., 2015; Tremper et al., 2022), and flight activity (Chung et al., 2023; Hsu et al., 2013; Hudda et al., 2016).

Other studies have evaluated the separate contributions from airport and road traffic emissions to total UFP concentrations, to find either comparable contributions (Austin et al., 2021; Masiol et al., 2016; Tremper et al., 2022) or higher contributions from airports compared to traffic (Shirmohammadi et al., 2017; Stacey et al., 2020). In Copenhagen, UFP concentrations measured at the apron of Copenhagen Airport were reported to be two to three times higher than those measured at a high-traffic street in the city centre (H.C. Andersens Boulevard) in 2012 (Ellermann et al., 2012). Another Danish study equipped members of different occupational groups at Copenhagen Airport with mobile monitoring instruments and assessed their UFP exposure, finding seven times higher average concentrations for baggage handlers compared to employees mainly working indoors (37,000 versus 5,000 p/cm³, respectively) (Møller et al., 2014). Finally, a more recent study combined mobile monitoring by a Google Street View car with modelling approaches to estimate UFP concentrations for all streets in Copenhagen, Frederiksberg and Tårnby municipalities (Kerckhoffs et al., 2022). The resulting exposure map shows clearly elevated UFP concentrations in the residential areas bordering Copenhagen airport to the west and north, with higher concentrations than in other residential areas in the city.

2.3. Study objectives

We aimed to map UFP concentrations in a residential area in the vicinity of Copenhagen airport using a cyclist, who is moving through, in a near airport neighbourhood which may be characterized by large spatial variations according to distance from emission sources (e.g., motorized air and road traffic) as well as street and building typology. Specifically, we performed it in the near airport neighbourhood of Amager, Copenhagen, Denmark, which includes a municipality-run regulatory UFP monitoring station (*Backersvej station*), for which our mobile measurements were compared against by intermittent co-location. We aimed to perform our mobile measurement (cycling) campaign twice per weekday, in periods of the day (~08:15h and ~12:00h) for which regional wind pattern is expected to change, for twenty-two repeats of each in total. We further aimed to evaluate UFP exposure concentrations at a beach-side 'blue space' (*Amager Strandpark*) route, not previously studied; this build upon a previous (unpublished) study of a 'green space' path, showing substantially reduced UFP concentrations.

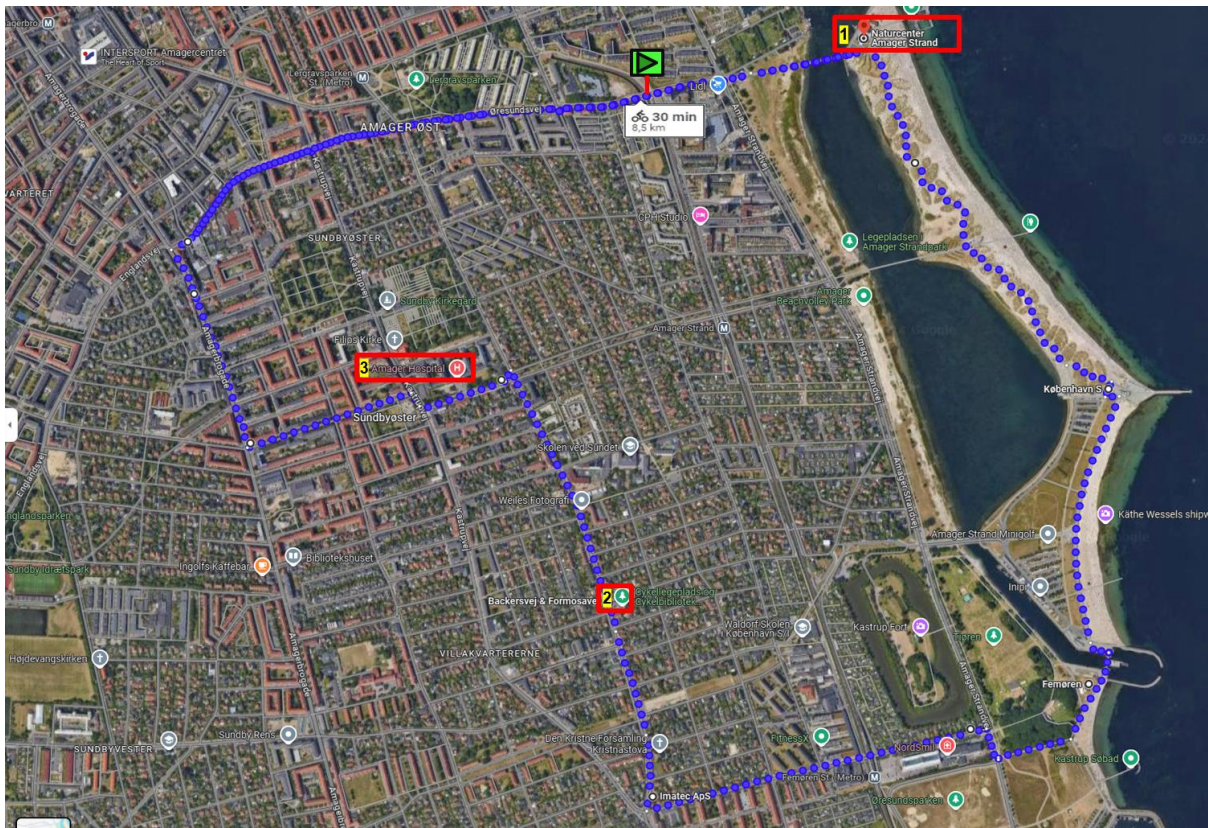
3. Study methods

3.1. Study setting

Across seven consecutive weeks during the months of July and August 2024, 44 cycling trips were conducted on a fixed route of ~8.5 km in Copenhagen (see Figure 1, next page, with route running clockwise):

1. Starting at intersection of Krimsvej and Øresundsvej, at Øresund metro station (📍);
2. Continuing eastward to Amager Strand [¹];
3. Turning southward at Nature Centre Amager Strand;
4. Continuing southward down Amager Strand, past Amager Strand Skatepark;
5. Turning westward along Hedegaardsvej past Femøren metro station;
6. Turning northward along Backersvej and continuing north past Backersvej monitoring station, at the intersection of Backersvej and Formosavej [²];
7. Turning westward again past Amager Hospital to Amagerbrogade [³];
8. Turning northward again along Amagerbrogade to Øresundsvej;
9. Turning eastward again towards and past Lergravsparken;
10. Ending at Øresund metro station, at intersection of Krimsvej and Øresundsvej.

Figure 1. Study route (total length ~8.5 km) performed twice per day at 08:15h and 12:00h for 22 repeats each.



Note: 1. Corresponds to Amager Strandpark; 2. Corresponds to monitoring station; 3. Corresponds to Amager Hospital

Image credit: Google Maps

Trips lasted approximately 40 minutes and started at 8:15h ('morning') on weekdays in order to cover typical times of commutes to and from work, as well as an additional trip at 12:00h ('noon') in order to observe UFP concentrations when regional weather patterns (namely wind direction and speed) typically change. One member of the project team (Gonzalo Hevia-Ramos) completed all cycling trips, which ensured consistency of conduct.

3.2. Study methods

3.2.1. Ultrafine particle monitoring

A Testo 'DiSCmini' handheld nanoparticle counter (Testo SE & Co. KGaA, Germany) was used to measure UFP number and size in the cyclist's breathing zone at 1-second intervals. The DiSCmini measures particle number concentration (PNC) of particles with 10-300 nm in diameter of up to 1 million pt/cm³. Before each trip, the DiSCmini was zero-checked with a HEPA filter, to ensure that the instrument was not drifting in measurement accuracy and therefore consistency across all trips. To spatially assign UFP data, concurrent global positioning satellite (GPS) data was recorded with a GPS watch ('Forerunner 920XT'; Garmin Ltd., USA). Measurements were not done on days or at times with

rain/precipitation or high humidity because the DiSCmini, according to the manufacturer's instructions, does not provide reliable data at a humidity above 90%.

While, no formal limit values exist for UFP, insights on the UFP level variations in a neighbourhood near Copenhagen airport (i.e., Amager) can be gained to a limited extent by one fixed monitoring station (Force Technology, 2024). This station, measuring UFP since 2020, is a background station at the intersection of Backersvej and Formosavej (Force Technology, 2024). Figure 2 (below) shows the air pollution monitoring station at Backersvej (Figure 2.a).

A comparison of UFP concentrations from the DiSCmini was made with the Backersvej municipal-run UFP monitoring station. Backersvej data was collected from station management, for the entirety of the mobile monitoring campaign (July to August), with a co-location effort in July and October 2024 (Figure 2.b).

Figure 2. Backersvej station: (a) view from street, with Cykellegeplads in background and; (b) view towards street, at July co-location with DiSCmini, with roadworks.

(a)



(b)

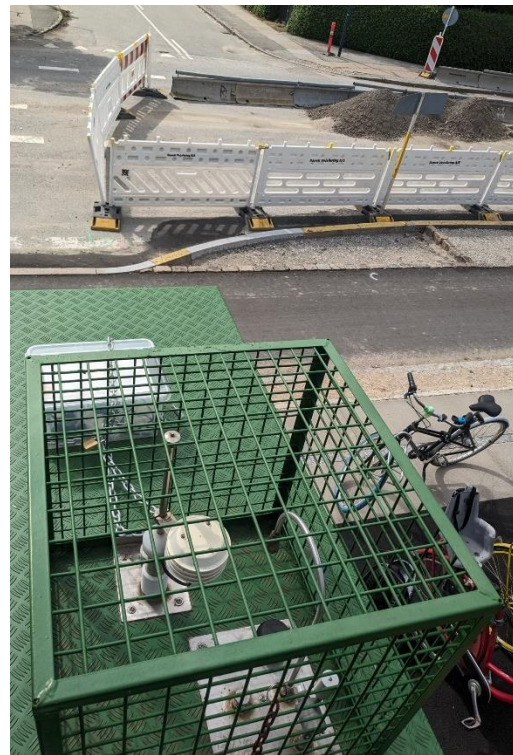


Image credit: (a) Google Street View; (b) own photo

3.2.2. Meteorological monitoring

To account for the influence of meteorological factors on UFP concentrations, which the existing literature and our previous studies have identified as important predictors of variation, we adjusted the measured PNCs for temperature, humidity and wind speed as done previously (Bergmann et al., 2022, 2021). Both of these meteorological factors have been seen as inversely related to UFP concentrations, with an increase in temperature and wind speed leading to a lowering of UFP concentrations (Hatzopoulou et al., 2013; Peters et al., 2014; Thai et al., 2008). An increase in wind speed, coupled with mixing layer height from a higher temperature inversion, leads to more favourable dispersion conditions (often seen in the afternoon) and better dispersion and dilution of locally-emitted pollutants (Hofman et al., 2018). Wind direction has been previously reported as influencing UFP concentration patterns in distant residential areas of a large commercial airport (Dröge et al., 2024). Therefore, we further considered wind direction observations for the study period, to characterize its influence on the UFP concentrations on the study route.

3.2.3. Airport flight information

To further understand air traffic, we requested air flight control information from Danish Civil Aviation and Railway Authority (*Trafikstyrelsen*), including actual landing and take-off date and time (i.e., when the wheels leave and touchdown on the runway [in Universal Time Constant]), the runway used (see Figure 3 below), and aircraft type.

Figure 3. Copenhagen Airport (CPH) runway orientation.



Image credit: Københavns Lufthavne A/S < <https://cph.flight-analyzer.casper.aero/content/2/Runwayuse/> >

3.2.4. Statistical analysis

We performed a Spearman¹ correlation test between the data collected from both co-locations of the DiSCmini and Backersvej station on the 24-25th of July and 3-4th October 2024, using five minutes PNC averages during a 24-hours period for both.

Temperature, humidity, wind speed and wind direction were obtained from the Danish Meteorological Institute (DMI) and means were calculated for the respective trip times. To analyse the differences between trips (morning vs noon) and between wind directions, we conducted two separate analyses using Generalized Additive Models (GAM), where PNC was controlled for mean temperature, mean wind speed, mean humidity, wind direction, date, and trip (morning/noon) (Figure A1, Appendix).

For spatial analysis, average PNC (combined for all trips across both time periods [morning and noon]) along the route was analysed by merging DiSCmini data with GPS data in R using package *ggspatial*. Points along the route were created each 30 meters, to which the mean values of all readings within a 20-meter radius around that point were assigned and aggregated. Additional spatial data, such as locations of traffic lights were retrieved from OpenStreetMap (OSM). Further analysis was performed aggregating PNC by wind direction for southerly, easterly and westerly wind. North wind was not considered as only one measurement was performed with north wind, and little aggregated data limited the interpretation.

¹ A Spearman correlation-test is a non-parametric test that is used to measure the degree of association between two variables. The test assumes a monotonic relationship between two variables, meaning that a resulting correlation coefficient of 1, or 100%, would resemble a perfect monotone function of each variable with the other. The p-value gives the chance of receiving the given result, if the null-hypothesis, meaning no association between the variables, were true.

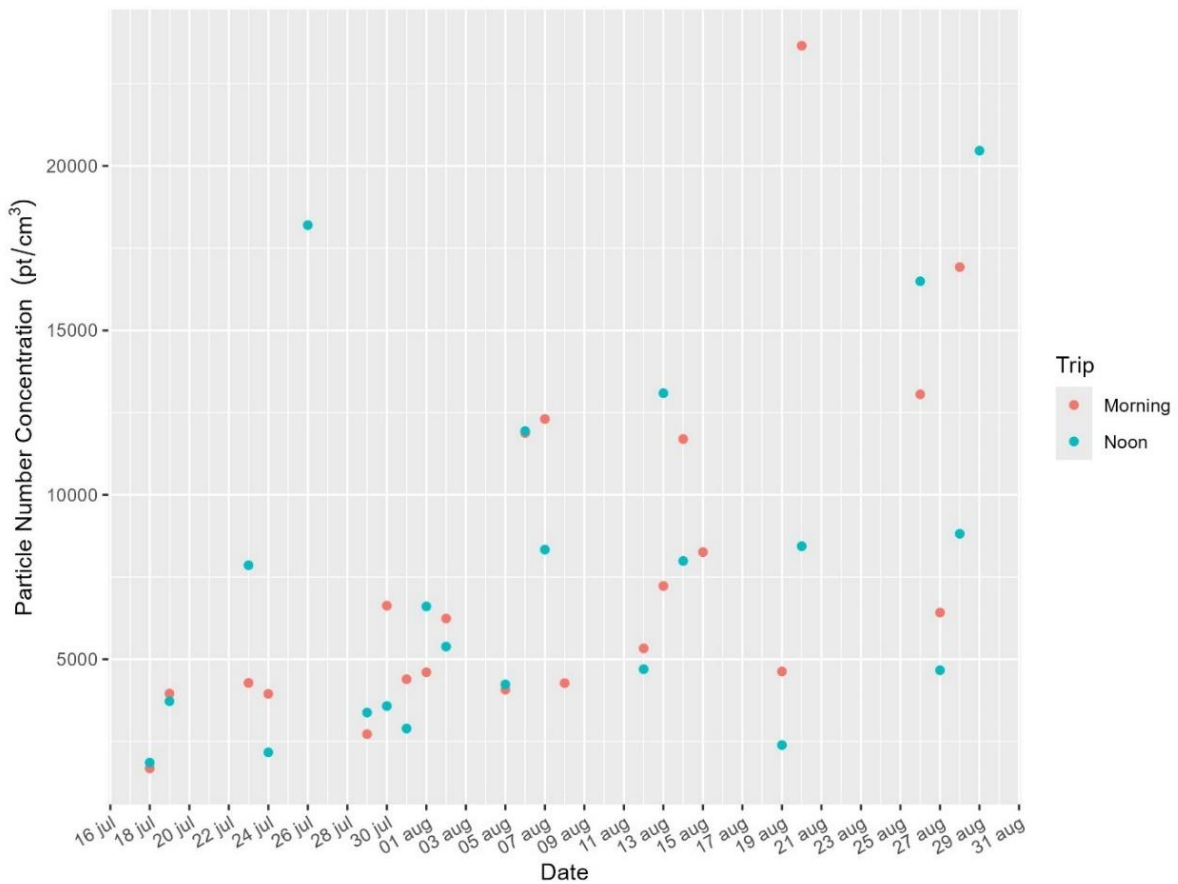
4. Results: Temporal patterns of ultrafine particle concentration

In our analysis of the data from the co-located DiSCmini next to the Backersvej monitoring station, we found that 5-minute-average UFP concentrations measured by the two different instruments were highly correlated with 93% and 95% of agreement (Spearman correlation test, $p < 2.2e^{-16}$) for the first and second co-location, respectively. Despite differences in mean PNC, DiSCmini and station data were closely correlated, meaning that days or times with higher background PNC measured by the stations resulted in higher PNC measured along the cycling route.

Comparing the daily mean PNC across the different dates of trip performance, we observe large day-to-day variation in concentrations; however lower variations are observed within morning and noon trips during the same day (e.g. 18th July, 21st July, 5th August, 27th August) (Figure 4).

Our study measurements were only conducted over July and August, which partly coincides with local summer holidays and therefore reduced road traffic peaks (namely morning); yet, we have seen that flight traffic does vary throughout the year. The number of flights to and from Copenhagen Airport can fluctuate through the year and be highest in July and October, coinciding with summer and autumn holidays (Copenhagen Airport Guide, 2024). Therefore, flight numbers or airport activity could have been at its highest during our study period. Moreover, as the study period was during the warmest months of the year, people may tend to spend more time outdoors which may increase their exposure to UFP as measured (outdoors) in this study. That is to say, in combination, that our results may reflect the maximum UFP exposure concentrations possible for this area of study.

Figure 4. Daily mean PNC per trip period (morning, noon) on 24 weekdays during the study period (18/07/24–29/08/24).



Abbreviations: jul, July; aug, August.

Total mean PNC was 7,620 pt/cm³, ranging from 1,679 to 23,656 pt/cm³. There was no significant difference in UFP concentrations between the two time periods of the day, when adjusted for temperature, wind speed, wind direction and humidity (ANOVA-test $p=0.86$). The mean PNC for each trip was 7,643 pt/cm³ and 7,598 pt/cm³ during morning and noon, respectively (Table 1 & Table 2). Particle size was similar during both trips, adjusted for temperature, wind speed, wind direction and humidity (ANOVA-test $p=0.39$), which indicates similar traffic patterns and emission source contributions at different times of the day; for example, similar vehicle numbers and types according to amount and type of fuel combusted.

Table 1. Summary of overall PNC and particle size from 44 measurements on 24 weekdays during the study period (18/07/24–29/08/24).

Measurement	Mean	SD	Min	5th pctl.	25th pctl.	Median	75th pctl.	95th pctl.	Max
PNC (pt/cm ³)	7,620	5,269	1,679	2,200	4,043	5,809	9,534	18,009	23,656
Particle Size (nm)	47	12	10	30	39	48	53	66	67

Abbreviations: pt/cm³, particles per cubic centimetre of air; nm, nanometre; SD, standard deviation; Min, minimum value; Max, maximum value; pctl., percentile.

Table 2. Summary of overall PNC and particle size per trip (Morning & Noon) from 44 measurements on 24 weekdays during the study period (18/07/24–29/08/24).

Measurement	Trip	Mean	SD	Min	5th pctl.	25th pctl.	Median	75th pctl.	95th pctl.	Max
PNC (pt/cm ³)	Morning	7,643	5,300	1,679	2,781	4,273	5,783	10,834	16,731	23,656
PNC (pt/cm ³)	Noon	7,598	5,363	1,856	2,178	3,611	5,994	8,720	18,115	20,463
Particle Size (nm)	Morning	45	12	10	29	39	46	52	63	67
Particle Size (nm)	Noon	49	12	28	34	39	50	57	66	66

Abbreviations: pt/cm³, particles per cubic centimetre of air; nm, nanometre; SD, standard deviation; Min, minimum value; Max, maximum value; pctl., percentile.

Grouping PNC and particle size by four wind directions; to the north (northerly, N), east (easterly, E), south (southerly, S) and west (westerly, W) with one, eight, seventeen and eighteen trips for each group respectively, we observed the highest mean PNC of 11,594 pt/cm³ and smallest mean particle size of 44 nm for southerly wind. Higher concentration mean PNC 7,069 pt/cm³ were also found for easterly wind compared to northerly and westerly wind. Lower concentrations were observed for northerly wind, mean PNC 6,236 pt/cm³ with mean particle size 47 nm, and for westerly wind, PNC 4,189 pt/cm³ with mean particle size 50 nm (Table 3). The smaller mean particle size attributable to the southerly wind may be that the combustion of air traffic fuel generally produces smaller particles compared to road traffic fuel. Aircraft engines emit a significant amount of non-volatile particulate matter (nvPM), which includes black carbon and metal ash, as well as volatile particulate matter (vPM) like volatile organic compounds, nitrates, and sulphates (Corbin et al., 2022). These particles are typically smaller in size, often in the ultrafine range (less than 100 nanometres). In contrast, road traffic fuel combustion tends to produce larger particles. While road traffic also emits fine particles (PM_{2.5}), it contributes more significantly to larger particle sizes (PM_{2.5-10} and PM₁₀₋₂₀) due to factors like tire and brake wear, and road dust (Wang et al., 2024).

Table 3. Summary of overall PNC and particle size grouped by wind direction from 44 measurements on 24 weekdays during the study period (18/07/24–29/08/24).

Measurement	Trips	Mean	SD	Min	5th pctl.	25th pctl.	Median	75th pctl.	95th pctl.	Max
N										
PNC (pt/cm ³)	1	6,236	NA	6,236	6,236	6,236	6,236	6,236	6,236	6,236
Particle Size (nm)	1	47	NA	47	47	47	47	47	47	47
E										
PNC (pt/cm ³)	8	7,069	4,999	2,388	2,804	3,683	5,039	8,959	15,158	16,925
Particle Size (nm)	8	48	10	36	36	39	50	53	62	66
S										
PNC (pt/cm ³)	17	11,594	5,504	4,277	4,586	7,857	11,693	13,089	21,102	23,656
Particle Size (nm)	17	44	12	28	29	35	42	51	66	67
W										
PNC (pt/cm ³)	18	4,189	1,709	1,679	1,829	3,012	4,152	4,619	6,871	8,257
Particle Size (nm)	18	50	13	10	30	45	52	58	65	65

Abbreviations: N, northerly wind; E, easterly wind; S, southerly wind; W, westerly wind; pt/cm³, particles per cubic centimetre of air; nm, nanometre; SD, standard deviation; Min, minimum value; Max, maximum value; pctl., percentile.

Further analysis was conducted using eight wind directions: northerly (N), northeasterly (NE), easterly (E), southeasterly (SE), southerly (S), southwesterly (SW), westerly (W), and northwesterly (NW), with one, two, three, fifteen, five, one, thirteen and fourth trips for each wind direction respectively. The highest mean PNC were also found for southerly wind (13,067 pt/cm³) with a mean particle size of 48 nm. The smallest mean particle size was found for southeast wind, with 42nm, with high mean PNC of 11,237 pt/cm³. North wind and southwest wind had similar patterns, with mean PNC of 6,236 pt/cm³ and 6,417 pt/cm³ respectively, both with a mean particle size of 47 nm. Smaller mean PNC and higher particle size were found for northeasterly, easterly, and northwesterly winds, mean PNC 4,135 pt/cm³, 3,830 pt/cm³, 4,135 pt/cm³ and 3,479 pt/cm³, and mean particle size 52nm, 53nm and 53nm respectively (Table 4).

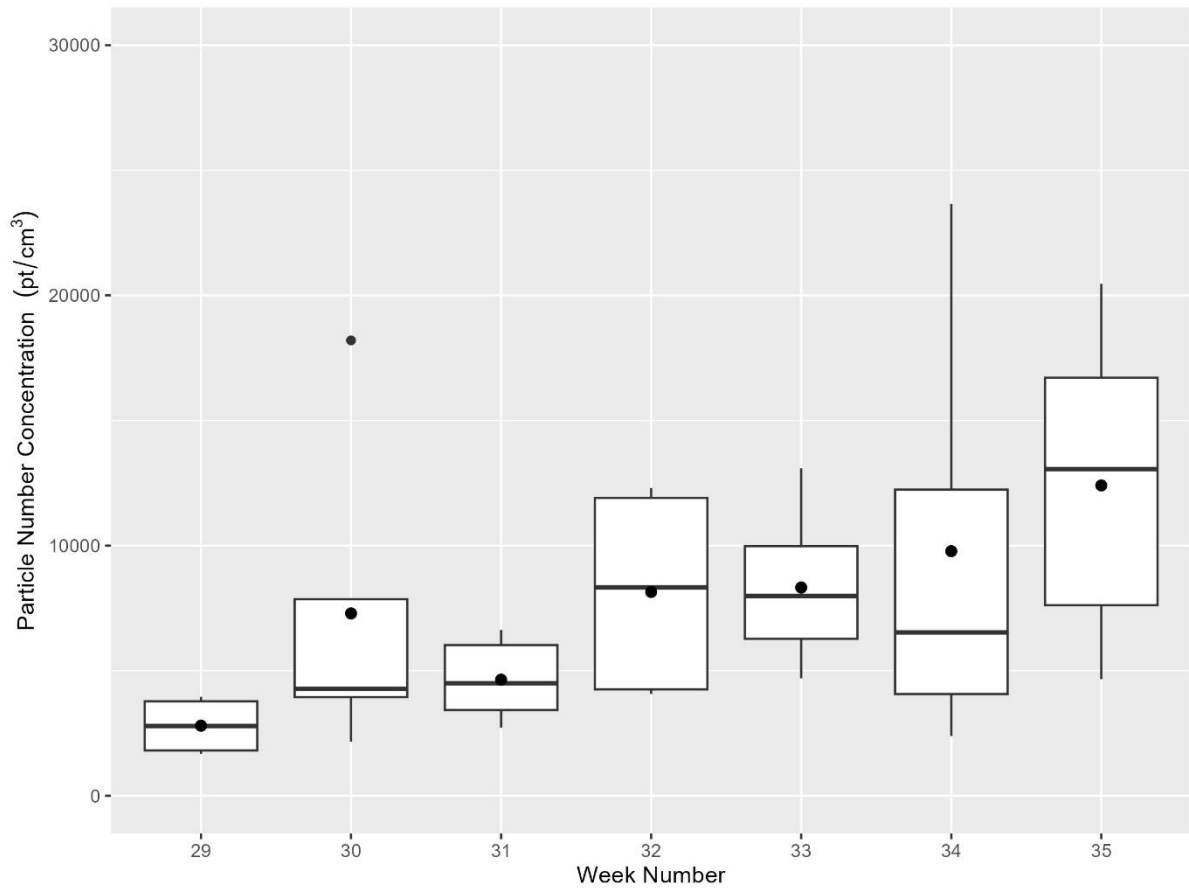
Table 4. Summary of overall PNC and particle size grouped by wind direction on 24 weekdays during the study period (18/07/24–29/08/24).

Measurement	Trips	Mean	SD	Min	5th pctl.	25th pctl.	Median	75th pctl.	95th pctl.	Max
N										
PNC (pt/cm3)	1	6,236	NA	6,236	6,236	6,236	6,236	6,236	6,236	6,236
Particle Size (nm)	1	47	NA	47	47	47	47	47	47	47
NE										
PNC (pt/cm3)	2	4,135	792	3,575	3,631	3,855	4,135	4,414	4,638	4,694
Particle Size (nm)	2	52	20	38	39	45	52	59	64	66
E										
PNC (pt/cm3)	3	3,830	1,500	2,388	2,522	3,054	3,719	4,551	5,217	5,383
Particle Size (nm)	3	53	3	51	51	51	52	54	56	56
SE										
PNC (pt/cm3)	15	11,237	4,513	4,664	6,022	8,158	11,693	12,696	18,879	20,463
Particle Size (nm)	15	42	8	28	32	36	40	48	54	57
S										
PNC (pt/cm3)	5	13,067	7,554	4,277	4,993	7,857	13,054	16,492	22,223	23,656
Particle Size (nm)	5	48	18	29	30	35	44	66	67	67
SW										
PNC (pt/cm3)	1	6,417	NA	6,417	6,417	6,417	6,417	6,417	6,417	6,417
Particle Size (nm)	1	47	NA	47	47	47	47	47	47	47
W										
PNC (pt/cm3)	13	4,237	1,843	1,679	1,785	3,377	4,272	4,625	7,279	8,257
Particle Size (nm)	13	49	15	10	24	44	52	60	64	65
NW										
PNC (pt/cm3)	4	3,479	784	2,719	2,745	2,848	3,481	4,112	4,208	4,232
Particle Size (nm)	4	53	9	44	45	49	51	56	64	65

Abbreviations: N, northerly wind; NE, northeasterly wind; E, easterly wind; SE, southeasterly wind; S, southerly wind; SW, southwesterly wind; W, westerly wind; NW, northwesterly wind; pt/cm3, particles per cubic centimetre of air; nm, nanometre; SD, standard deviation; Min, minimum value; Max, maximum value; pctl., percentile.

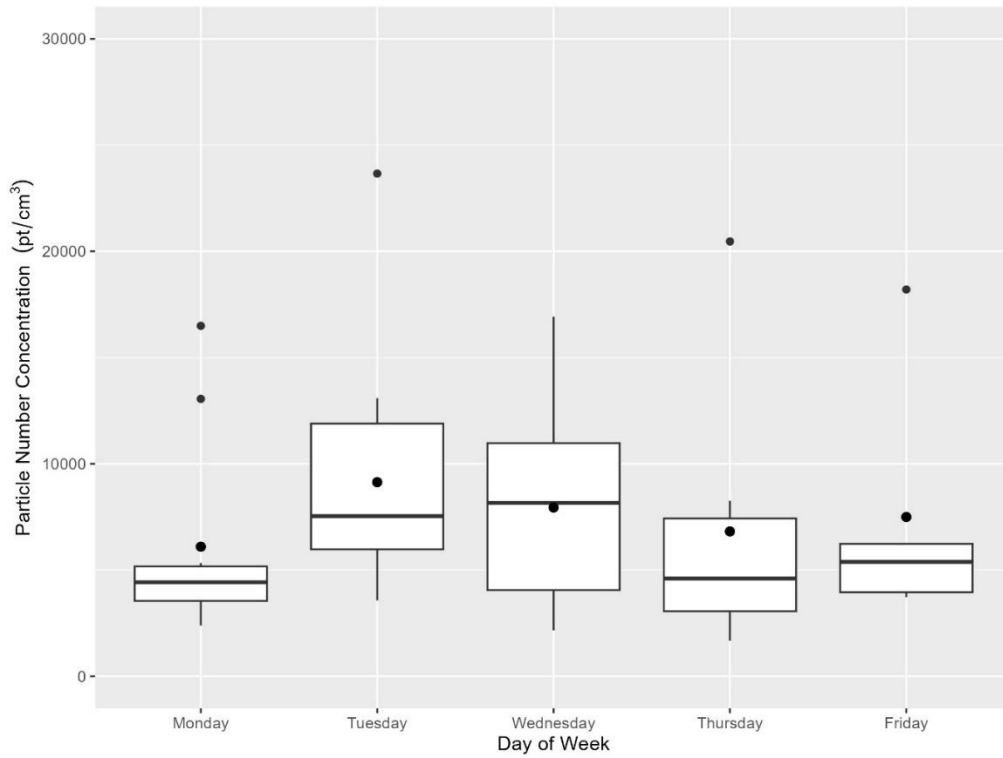
We analysed all trip data (all days, both time periods) for PNC by week number during the study period (Figure 5, below). From this, we noticed an increasing trend in UFP concentrations during the study period, especially in week 32 and week 35. This is likely to be explained by the increase in frequency of southerly wind in week 32 and 35 (Figure 5).

Figure 5. Boxplot showing weekly PNC (morning and noon trips combined) from 44 measurements on 24 days during the study period (18/07/24–29/08/24) by week of the year for study duration. During week numbers 29-35, the number of trips per week were 4, 5, 10, 7, 7, 4 and 7, respectively.



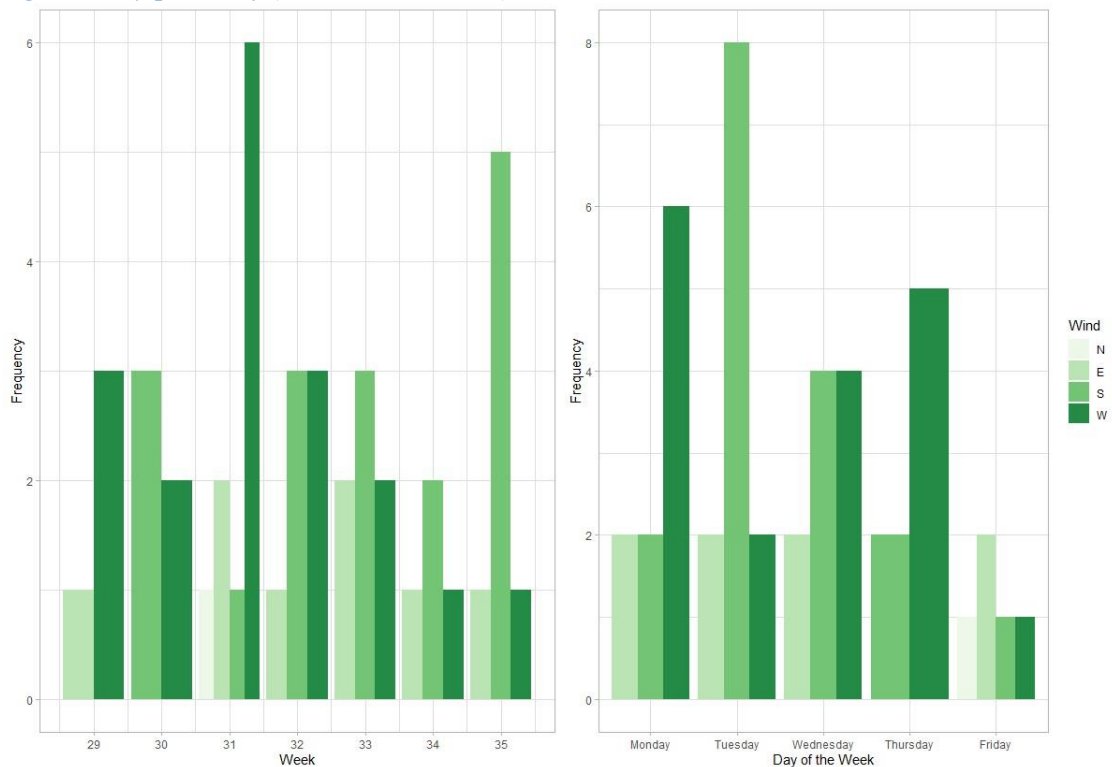
Further, we analysed all trip data (all days, both time periods) for PNC by day of week (Figure 6, below). From this, we see noticeably higher mean and median PNC on Tuesdays and Wednesday. As for the week number, this could be explained by the higher frequency of southerly wind on Tuesdays and Wednesday during the study period (Figure 7, below).

Figure 6. Boxplot showing daily PNC (morning and noon trips combined) from 44 measurements on 24 days during the study period (18/07/24–29/08/24) by day of the week. On Mondays to Fridays, a total of 10, 12, 10, 7 and 5 trips were done, respectively.



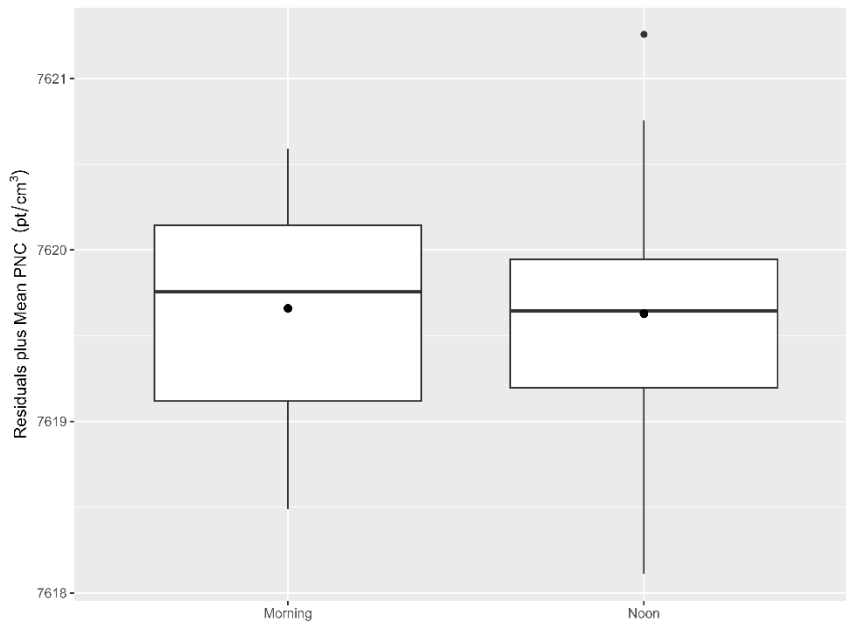
Abbreviations: pt/cm³, particles per cubic centimetre.

Figure 7. Distribution (histogram) of Frequency for wind directions per week and day of the week during the study period of (18/07/24–29/08/24).



After adjustment for meteorological factors (wind direction, wind speed, temperature and humidity), time trend, trip (morning & noon), and device of measurement, using a GAM, the two trip periods were still not significantly different (Figure 8, below).

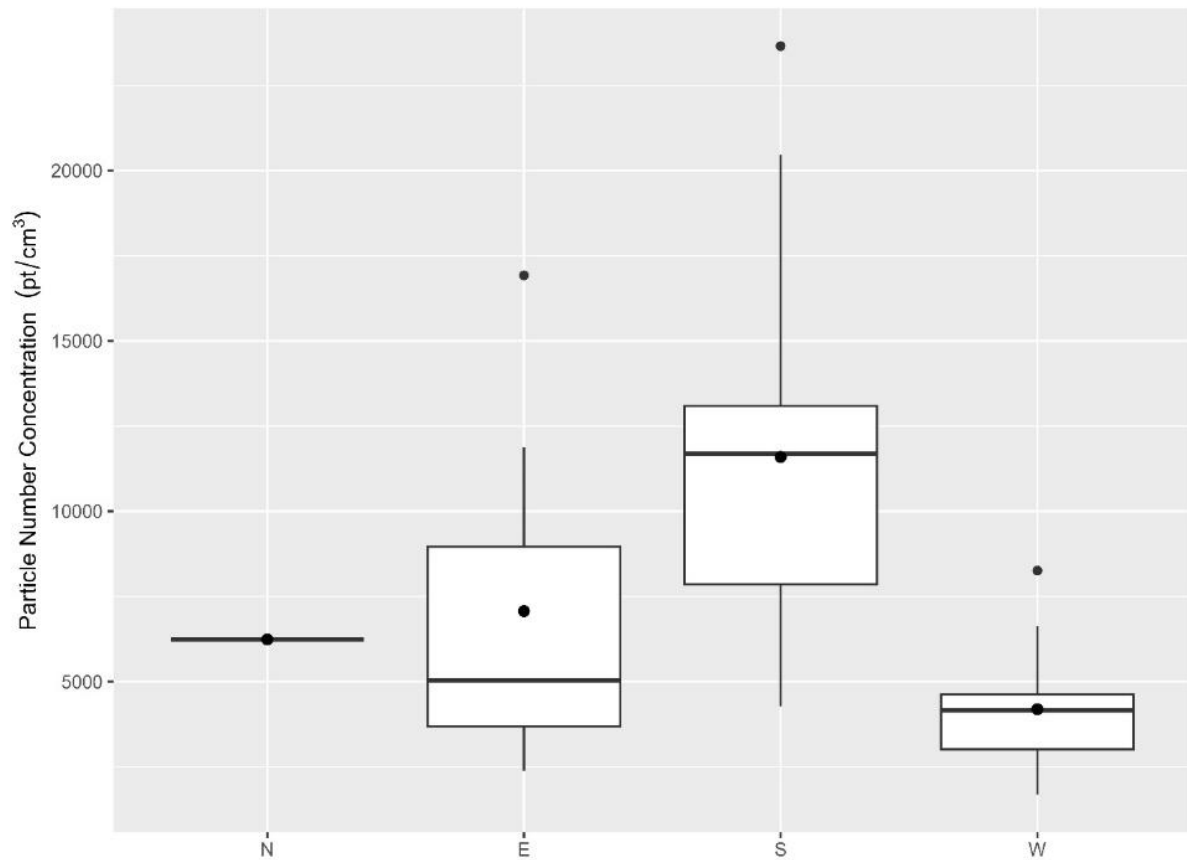
Figure 8. Boxplot with Residuals plus mean PNC on 24 weekdays from 44 measurements during the study period (18/07/24–29/08/24), for morning (8:15-9:00) and noon (12:00-12:45), adjusted by the effects of wind direction, wind speed, temperature, humidity, time trend and device of measurement, using Generalized Additive Model.



Abbreviations: pt/cm³, particles per cubic centimetre.

Non-adjusted PNC are presented in Figure 9, below. We observed higher median concentrations when measurements were done with southerly wind (~12,000 pt/cm³), followed by northerly wind (~6,000 pt/cm³), easterly wind (~5,000 pt/cm³), and westerly wind (4,000 pt/cm³).

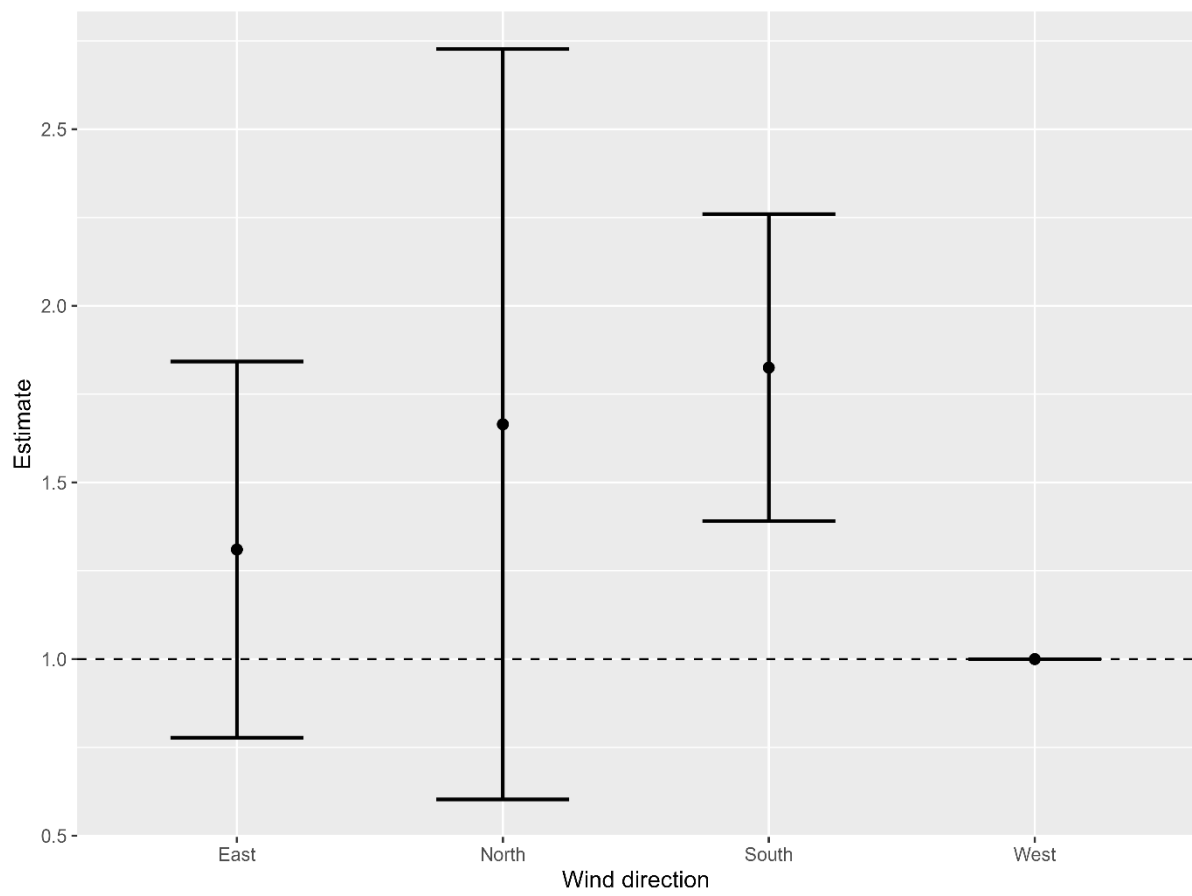
Figure 9. Boxplot showing overall PNC (morning and noon trips combined) from 44 measurements on 24 days during the study period (18/07/24–29/08/24) by wind direction. North, east, south and west wind directions, with a total of 1, 8, 17, and 18 trips, respectively.



Abbreviations: N, north wind; E, east wind; S, south wind; W, west wind; pt/cm³, particles per cubic centimetre.

After adjustment for meteorological factors (wind speed, temperature and humidity), time trend, trip (morning & noon), and device of measurement, using a GAM, south wind direction impacted significantly in the PNC and was significantly higher than west wind (in average ~1.8 times higher, ranging from 1.4 to 2.3). Conversely, east and north wind direction showed higher but non-significant overall PNC compared to west wind direction (Figure 10).

Figure 10. Estimates (morning and noon trips combined) from 44 measurements on 24 weekdays during the study period (18/07/24–29/08/24), by wind direction, adjusted for the effects of wind speed, temperature, humidity, time trend and device of measurement, using Generalized Additive Model.

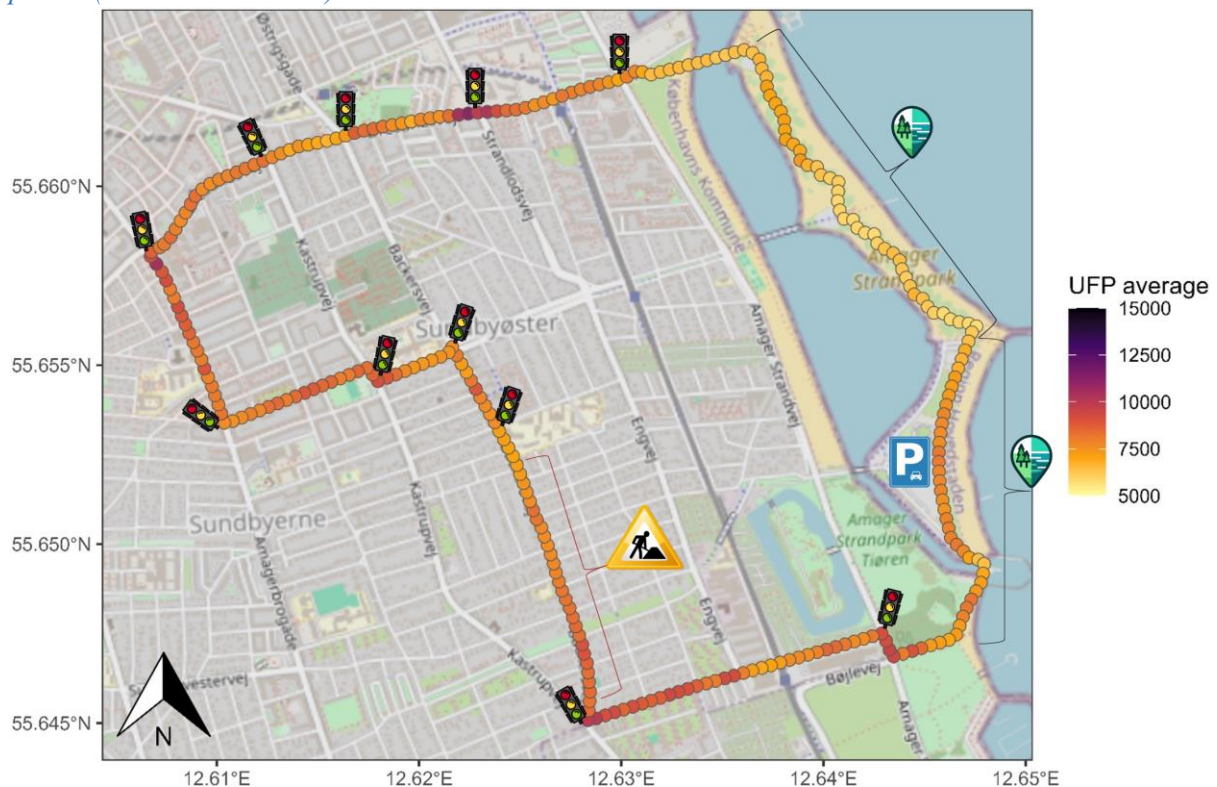


5. Results: Spatial patterns of ultrafine particle concentration

While mean PNC measured across the two morning time periods did not vary significantly, UFP concentrations measured across the many spaces varied substantially. This result in general is equivalent to what we saw in the previous study, for which we saw the importance of spatial ‘hotspots’ including traffic light in congested intersections and construction sites (Figure 11, below).

Figure 11 shows aggregated PNC (UFP concentrations) along the route across all trips, with lighter (e.g. yellow/orange) colours indications lower, and darker (e.g. purple/orange) indicating higher average of UFP concentrations. High PNC were found at segments of Amager Strandvej, Backersvej, Kastрупvej, Amagerbrogade and Strandlodsvej, and may be caused by traffic lights in congested crossings (~10,000-15,000 pt/cm³). Segments with lowest mean PNC were identified mainly at Amager Strandpark (~6,000 pt/cm³). Overall, these findings are in line with studies, which show that UFP concentrations can be influenced by traffic intensity and the built environment, namely street and building infrastructure (Berghmans et al., 2009; Boogaard et al., 2009; Luengo-Oroz and Reis, 2019; Peters et al., 2014). Higher concentrations were also measured in street canyons (Amagerbrogade, ~10,000 pt/cm³) and near construction sites (Backersvej, ~9,000 pt/cm³), but main UFP concentrations remains at traffic lights in congested streets.

Figure 11. Spatial aggregation of average UFP concentrations within a 20-meter radius around points every 30 meters (morning and noon combined) from 44 measurements on 24 weekdays during the study period (18/07/24–29/08/24).



Abbreviations: N, north direction; UFP, ultrafine particles (unit: pt/cm³). Image source: OpenStreetMaps.

Below we zoom in and give visual examples of the main areas of interest, such as traffic lights in congested streets, a construction zone, a ‘blue space’ (Amager Strandpark) and a health centre (Amager Hospital). These areas are of special interest due to expected higher (near to emission sources) and lower (far from emission sources) concentrations of UFP, or higher susceptibility of citizens (e.g. Amager Hospital).

As expected, average UFP exposure concentrations measured along Amager Strandpark, were lowest of the overall route, but only in the upper two third of the park route, approximately at 5,000 pt/cm^3 (Figure 12). For the lowest third of the Amager Strandpark route, we found higher average UFP concentrations, approximately at 7,500 pt/cm^3 (Figure 12). This might be explained by the upper two thirds of the Amager Strandpark being car free zones, and the lower third of the route characterized by car parking zones along the route, as presented below, as well as proximity to the airport (Figure 12).

Figure 12. Averages of ultrafine particles (UFP) at Amager Strandpark, Copenhagen.



Abbreviations: UFP, ultrafine particles (unit: pt/cm^3). Image (map) source: map, OpenStreetMaps; photo, GoPro footage.

Average UFP exposure concentrations measured within 30 m of intersections between main roads along the entire trip route were seen as “hotspots” for UFP exposure concentrations. At the intersection between Amager Strandvej and Hedegaardsvej higher UFP averages were seen, approximately 10,000 pt/cm³ (Figure 13).

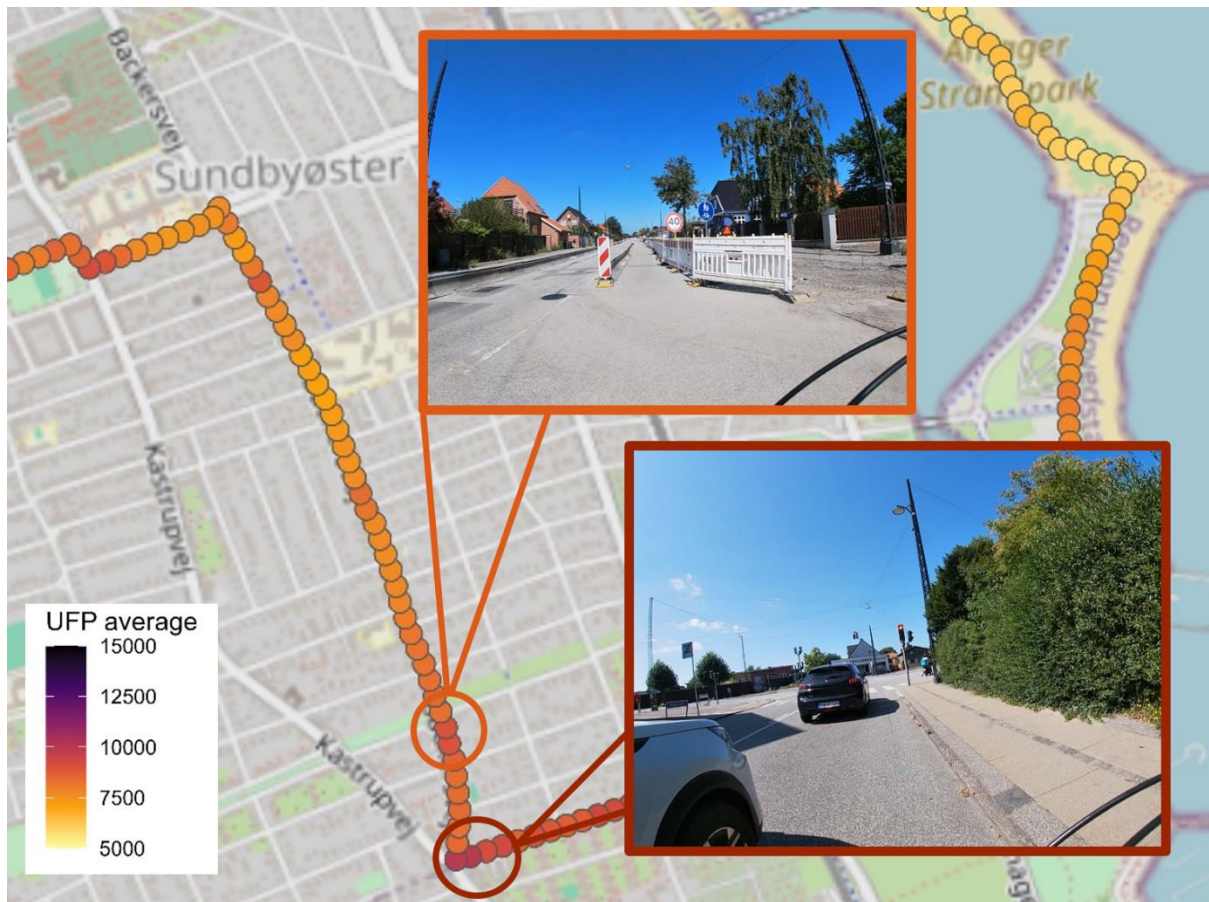
Figure 13. Averages of ultrafine particles (UFP) at Amager Strandvej intersection, Copenhagen.



Abbreviations: UFP, ultrafine particles (unit: pt/cm³). Image (map) source: map, OpenStreetMaps; photo, GoPro footage.

At the intersection between Hedegaardsvej and Backersvej, higher UFP average concentrations were also seen, approximately 10,000 pt/cm³ (Figure 14). At Backersvej, despite being a residential area, with low traffic, some higher concentrations were found along the route next to construction sites, with approximately UFP averages of 9,000 pt/cm³ (Figure 14). This is believed to be due to construction and heavy machinery (visible on the GoPro footage) found at these sites (Figure 14). Despite the increased UFP average concentrations at the construction sites, the road was unfrequently used by individuals.

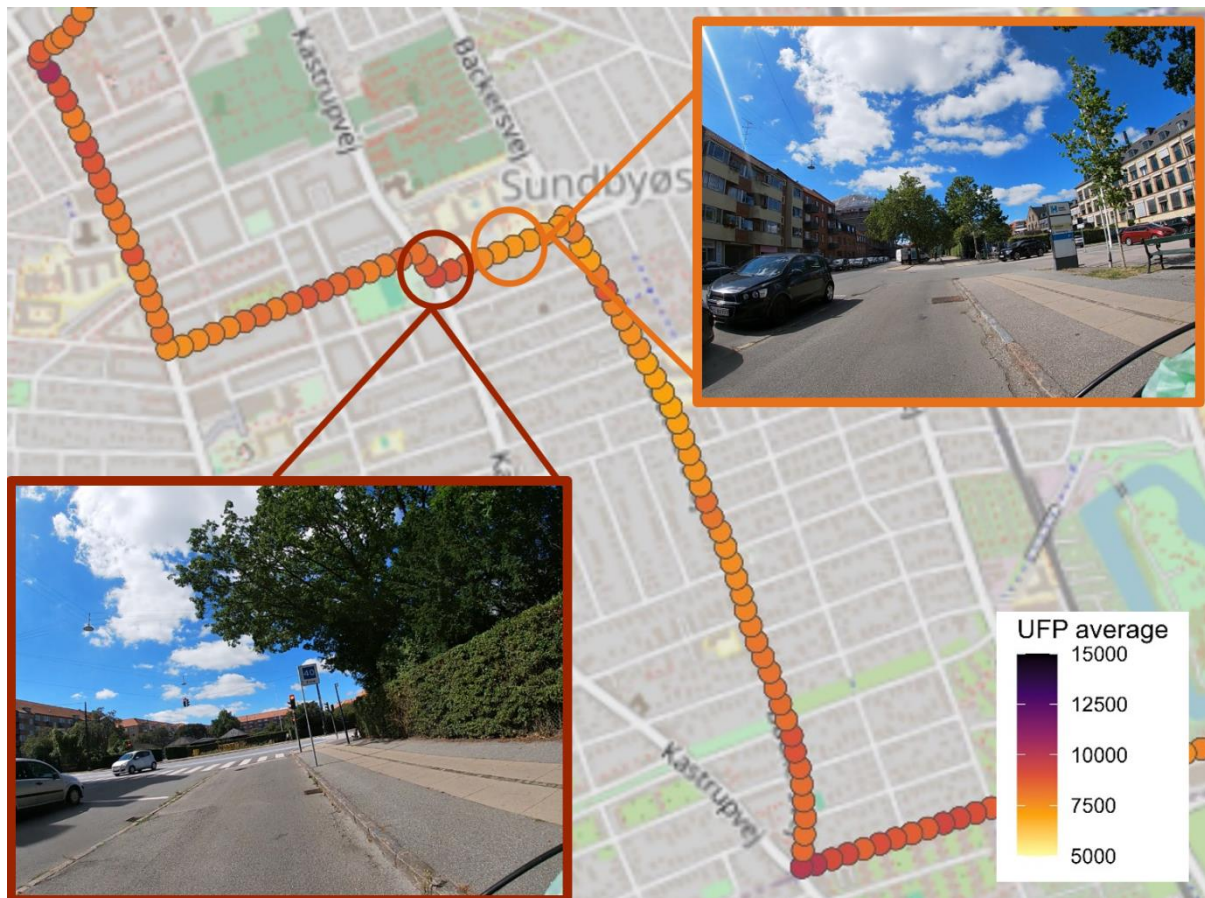
Figure 14. Averages of ultrafine particles (UFP) at Backersvej intersection and at construction site, Copenhagen.



Abbreviations: UFP, ultrafine particles (unit: pt/cm^3). Image (map) source: map, OpenStreetMaps; photo, GoPro footage.

Average UFP exposure concentrations measured along 30 m distances of Amager Hospital, were seen to be $\sim 7,500 \text{ pt}/\text{cm}^3$ (Figure 15). Next to Amager Hospital, at the intersection between Kastrupvej and Italiensvej, higher UFP averages were found, approximately $10,000 \text{ pt}/\text{cm}^3$.

Figure 15. Averages of ultrafine particles (UFP) at Amagerbro Hospital and closest traffic light, Copenhagen.



Abbreviations: UFP, ultrafine particles (unit: pt/cm^3). Image (map) source: map, OpenStreetMaps; photo, GoPro footage.

At the intersection between Amagerbrogade and Øresundsvej, which can be described as a street canyon, with a high presence of vehicles, high average UFP concentrations were found, approximately $12,000 \text{ pt}/\text{cm}^3$ (Figure 16).

Figure 16. Averages of ultrafine particles (UFP) at Amagerbrogade intersection.



Abbreviations: UFP, ultrafine particles (unit: pt/cm^3). Image (map) source: map, OpenStreetMaps; photo, GoPro footage.

At the intersection between Øresundsvej and Strandlodsvej, which is characterized by a high presence of vehicles, higher UFP average concentrations were found, $\sim 13,000 \text{ pt}/\text{cm}^3$ (Figure 17).

Figure 17. Average level of UFP at traffic lights of intersection on Øresundsvej and Strandlodsvej, Copenhagen.



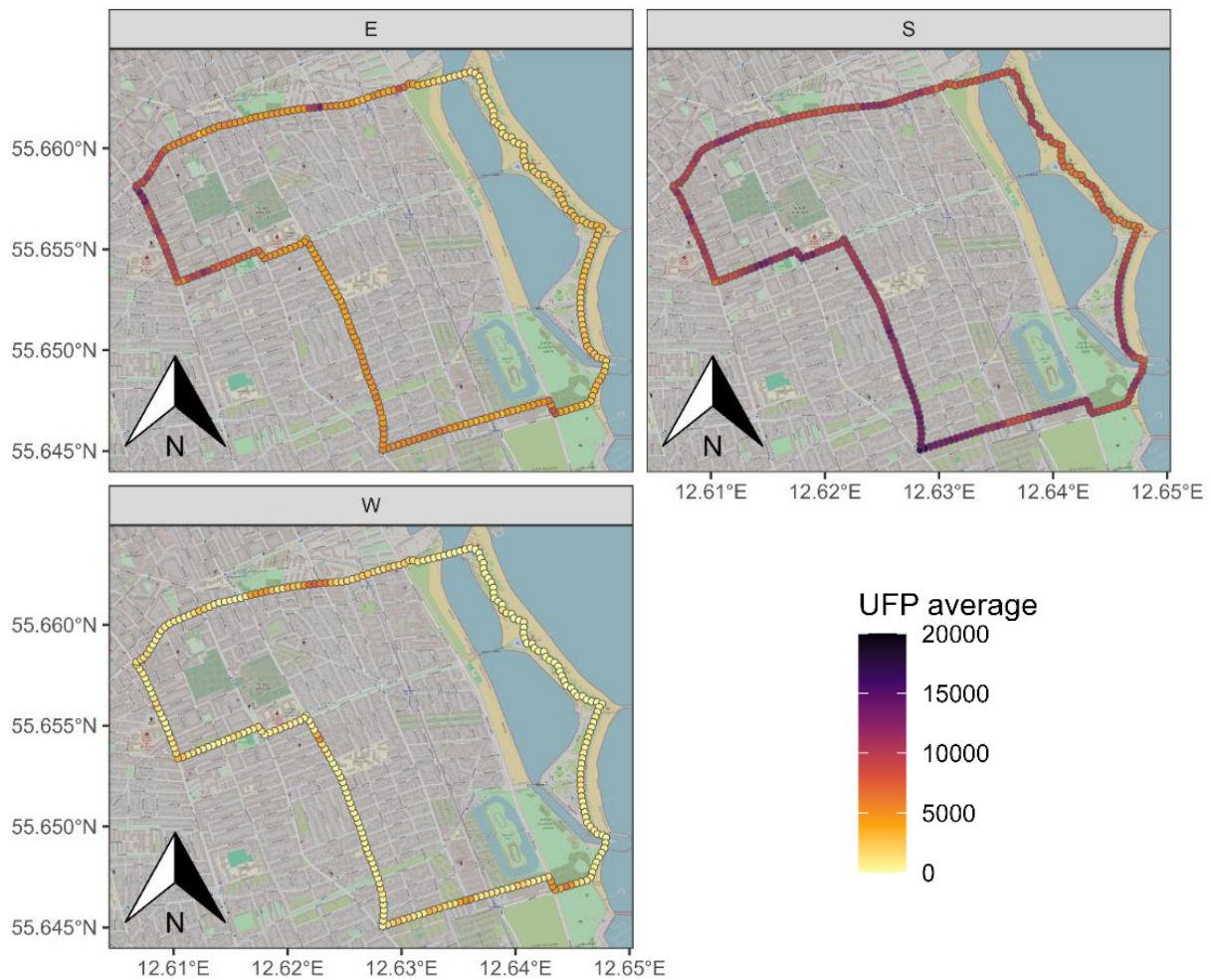
Abbreviations: UFP, ultrafine particles (unit: pt/cm^3). Image (map) source: map, OpenStreetMaps; photo, GoPro footage.

We further analyse the spatial aggregation of average UFP concentrations using 20- meter radius points every 30 meters of all 44 trips, grouped by wind directions (Figure 18). North wind was not considered as this wind direction was measured only once during our study. In addition, when analysing all four (south, west, east, north) wind directions, north wind data with very limited aggregation affected the overall scale, which made the interpretation difficult.

Interpreting the spatial aggregation grouped by wind directions, we found significant differences when comparing east, south and west winds (Figure 18). Measurements with south wind represented the highest UFP averages along the road $\sim 12,000 \text{ pt}/\text{cm}^3$, with visually increased UFP averages in the most southern route $\sim 15,000 \text{ pt}/\text{cm}^3$, and a less marked spatial variation between Amager Strandpark $\sim 10,000 \text{ pt}/\text{cm}^3$, and the rest of the route (Figure 18). With east wind, highest concentration of UFP averages were found along the route by Amagerbrogade $\sim 12,000 \text{ pt}/\text{cm}^3$ and high spatial variation was seen in Amager Strand Park, with lower concentrations of UFP averages $\sim 3,000 \text{ pt}/\text{cm}^3$ (Figure 18). With west winds, lower average UFP concentrations were seen in the overall route $< 5,000 \text{ pt}/\text{cm}^3$, with some mild

increases at the intersection points previously described, and a lower spatial variation between Amager Strandpark and the rest of the route (Figure 18).

Figure 18. Spatial aggregation of average UFP concentrations within a 20-meter radius around points every 30 meters (morning and noon combined) on 24 weekdays during the study period (18/07/24–29/08/24) grouped by wind direction.



Abbreviations: N, north direction; UFP, ultrafine particles (unit: pt/cm^3). Image source: OpenStreetMaps.

According to a report from the Danish Meteorological Institute, analyzing data from 1768 to 2020: north wind direction is the least frequent in Denmark; easterly wind is common during late winter and spring seasons; southerly wind is most common during autumn, and; westerly wind is the predominant wind direction in Denmark, with an increased frequency during summer (Cappelen, 2021). As for Copenhagen Airport, these wind patterns are reflective of Denmark at large (Figure 19).

Figure 19. Wind direction as a percentage of hours across the months of the year at Copenhagen Airport

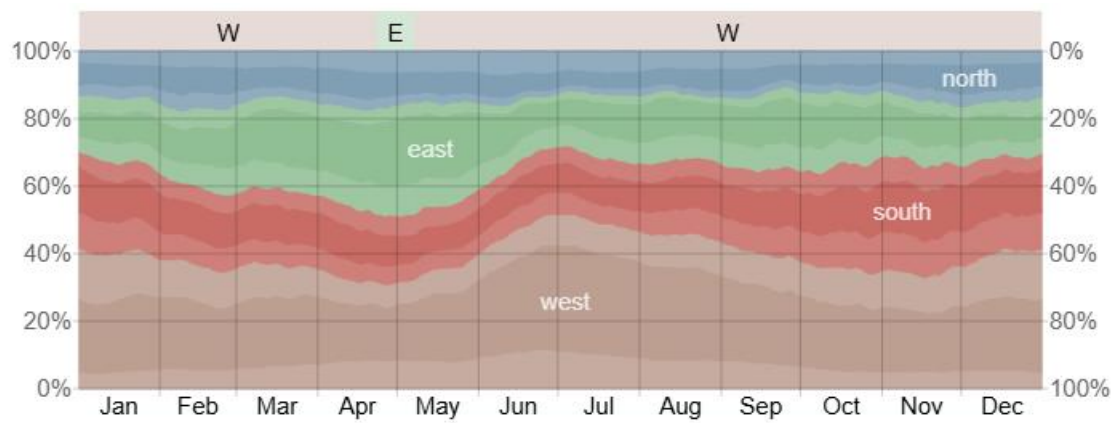


Figure source: Weather Spark < <https://weatherspark.com/y/148269/Average-Weather-at-Copenhagen-Airport-Denmark-Year-Round#Figures-WindDirection> > (“The percentage of hours in which the mean wind direction is from each of the four cardinal wind directions, excluding hours in which the mean wind speed is less than 1.0 mph. The lightly tinted areas at the boundaries are the percentage of hours spent in the implied intermediate directions (northeast, southeast, southwest, and northwest).”)

6. Comparison to other airport and city bicycling studies

6.1. Airport-related studies

While this is the first study to measure UFP exposure while cycling in a neighbourhood adjacent to an airport, including a route that is considered ‘blue space’, other studies have included mobile measurement campaigns of airport-related exposures: two in Berlin, Germany (Fritz et al., 2022; Gerling and Weber, 2023), and one in Warwick, USA (Hsu et al., 2014) (Table 5, below). In the immediate vicinity of Berlin-Tegel Airport, in summer of 2019, a median PNC of 11,200 pt/cm³ was found (Fritz et al., 2022). In residential suburbs surrounding T.F. Green International Airport (Warwick, USA), in both Spring and Summer of 2008, a median PNC of approximately 5,000 pt/cm³ was found (Hsu et al., 2014). The median PNC value of the current study, in a suburb adjacent to Copenhagen International Airport, is approximately 6,000 pt/cm³, which is within the range of the previously reported median values.

Airport studies using stationary measurement campaigns have found a range of median PNC values, from approximately 10,000 pt/cm³ in Downtown Los Angeles, USA (Choi et al., 2013), compared to approximately 50,000 pt/cm³ in a Los Angeles International Airport (LAX)-adjacent neighbourhood (Westerdahl et al., 2008). A similar story is told in the Netherlands, with PNC at approximately 10,000 pt/cm³ North or South of Schiphol Airport (Amsterdam), Netherlands (Lenssen et al., 2024a), compared to approximately 35,000 pt/cm³ adjacent to Schiphol Airport (Pirhadi et al., 2020). This suggests that proximity to major airports is a strong driver of UFP exposure; although, wind direction and speed may also be a strong driver of this. Two studies calculated a term to determine the size of contributions to PNC from airport activities, namely landing and takeoff (LTO) (Hsu et al., 2014; Hudda et al., 2018). The former study used a complex model (as a function of distance from roadway, landing and take-off (LTO) activity, and meteorology) to predict UFP concentrations (Hsu et al., 2014). This approach was able to demonstrate UFP contributions from major surrounding runways and LTO activity to UFP concentrations near a mid-sized airport, providing a methodology for source attribution within a community with multiple distinct sources. Specifically, that study made two important findings: (1) departures and arrivals on a major runway had a significant influence on UFP concentrations in a neighbourhood proximate to the end of the runway, with a limited influence elsewhere, and (2) mean traffic contributions exceed mean LTO contributions, but LTO activity can dominate the contribution during some minutes of the day (Hsu et al., 2014).

In our study, while bicycling, we found a major determinant of UFP concentrations to be wind direction with a median PNC of approximately 11,600 pt/cm³ when wind was from the south of measurement location. Conversely, with wind from the north, east or west of measurements, a median PNC of approximately 6,200 pt/cm³, 7,100 pt/cm³, and 4,200 pt/cm³, respectively, was observed. This was supported by our GAM model, in which despite adjusting for meteorological factors and time trends,

south wind showed to be consistently and significantly associated to higher PNC, than north, east and west winds.

In the current study, sections of the route closer to CPH airport were seen to be of a slightly higher exposure level for UFP when aggregated by south wind, compared to sections further from CPH airport. In addition, the all-trips route exposure level for UFP showed higher spatial variation than the aggregated route for south wind, which suggest an attenuation of the spatial variation affected by south winds.

6.2. City-related studies

6.2.1. Exposures at different times of day

Studies that have measured UFP exposure while bicycling have been conducted in Europe and North America (Table 6, below). Among them, some studies compare exposure at different times of the day (Berghmans et al., 2009; Hankey and Marshall, 2015; Hatzopoulou et al., 2013; Hofman et al., 2018; Kaur et al., 2005; Peters et al., 2014; Qiu et al., 2019; Ragetti et al., 2013). Seven studies conducted in Belgium, Canada, Switzerland, China and the UK found higher UFP concentrations during morning rush-hours compared to afternoon rush-hours (Berghmans et al., 2009; Hatzopoulou et al., 2013; Hofman et al., 2018; Kaur et al., 2005; Qiu et al., 2019; Ragetti et al., 2013; Yang et al., 2021). A few studies now have quantified exposure to UFP while bicycling in Copenhagen, at different time periods. The first was during weekday rush-hour commutes of 2005, which reported an average exposure of 32,400 pt/cm³ (Vinzents et al., 2005). Two more recent studies in Copenhagen have been published by the Environmental Epidemiology Group of University of Copenhagen. The first assessed UFP exposure concentrations while bicycling and walking inner-city routes during weekdays in the first half of 2020 (with COVID-19 restrictions implemented): bicycling occurred during the afternoon rush-hour, to show an average exposure of 11,963 pt/cm³ (Bergmann et al., 2021). In the second half of 2020 (when COVID-19 restrictions eased), for an equivalent afternoon rush-hour period, average UFP exposure concentrations were 17,569 pt/cm³ (Bergmann et al., 2022). These concentrations are markedly higher than the current study's average of approximately 7,600 pt/cm³ (combining both morning rush-hour [7,643 pt/cm³] and noon [7,598 pt/cm³] period values, due to their similarity), with the former results possibly attributable to being inner-city with major sources of UFP including congested road traffic. In a similar study in the mega-city of Beijing, China, average (peak and off-peak times combined) PNC were found to be approximately one-third higher than seen in Copenhagen when bicycling (Table 6) (Yang et al., 2021).

6.2.2. Exposures at different locations of city

Bicycling-specific studies have found increasing concentrations of UFP in relation to closer proximity to traffic (high- vs. low-exposure traffic routes) within a city (Cole-Hunter et al., 2012; Hankey and Marshall, 2015; Luengo-Oroz and Reis, 2019; Pattinson et al., 2017). While the magnitude of difference

in PNC due to spatial aspects such as major traffic corridors or intersections can be dependent on time of day, namely rush-hour traffic, other aspects are less so. Our previous studies in Copenhagen have seen an important determinant of PNC to also include the spatial aspects of bus stops, construction zones, and more recently green corridors. This observation has been repeated in the current study, although with a green corridor replaced by a ‘blue’ corridor, or route running along the sea (‘blue space’) with Amager Strand. For the green corridor, or route running through Nørrebroparken, an average of approximately 5,000 pt/cm³ was observed, which is equivalent to a large part of Amager Strand when wind is not coming from the south.

At Amager Hospital, as a point of interest due to critical health care, we saw PNC at approximately 10,000 pt/cm³. While no air quality guidelines for UFP from the WHO yet exist, should that concentration level remain on average over a 24-hr period, it would be considered concerning for health as listed in the WHO good practice statement: PNC levels of > 10,000 pt/cm³ as a 24-hr average, or > 20,000 pt/cm³ as a 1-hour average, should be considered high when making decisions on the control of source emissions (WHO, 2021).

At various traffic intersections in busy roads, as another point of interest due to high emission concentrations from congested road vehicles, we saw higher PNC at approximately 12,000 pt/cm³.

Bus stops in the current study followed a similar increased pattern in UFP to traffic intersections, as they were localised in the main roads which are characterised by higher concentrations of traffic, with average PNC of ~12,000 pt/cm³.

Table 5. Overview of studies on UFP exposure concentrations near airports

Authors, year	Study area	Total # of trips	Instrument, particle size range	Mean/Median PNC (pt/cm ³)	Type of exposure
Alzahrani et al. 2024	Madrid-Barajas Airport		CPC (10-100nm; <100,000 pcm ³)	Comparable metric not reported	At the airport perimeter during October 2021
Choi et al. 2013	Downtown Los Angeles		CPC (10-100nm; <100,000 pcm ³)	Median: 9,200-12,700	Different built environments of Boyle Heights (BH, a lower-income community enclosed by several freeways); Downtown Los Angeles (DTLA, adjacent to BH with taller buildings and surrounded by several freeways); and West Los Angeles (WLA, an affluent community traversed by two freeways) in summer afternoons of 2008 and 2011 (only for WLA)

Fritz et al. 2022	Berlin-Tegel Airport (TXL)	45 measurement runs took place along a 20–30 km route to the east of the airport	CPC (10-100nm; <100,000 pcm ³)	Median: 11,200	Mobile measurement campaign in the immediate vicinity of Berlin-Tegel Airport (TXL) in summer 2019
Gerling & Weber 2023	Berlin-Brandenburg airport (BER)	Eight days without rain and with western wind direction	CPC (10-100nm; <100,000 pcm ³)	Comparable metric not reported	Car-based mobile measurement campaign in the vicinity of the recently opened Berlin-Brandenburg airport (BER) in Germany
Hsu et al. 2014	T.F. Green International Airport (Warwick, RI, USA)		CPC (10-100nm; <100,000 pcm ³)	Median: ~5,000	Mobile monitoring campaign was conducted in five residential areas surrounding T.F. Green International Airport (Warwick, RI, USA) for one week in both spring and summer of 2008 *LTO*
Hu et al. 2009	Santa Monica Airport (SMA)		CPC (10-100nm; <100,000 pcm ³)	Median: ~25,000	
Hudda et al. 2018	Greater Boston metropolitan area (MA, USA) including Logan International Airport		CPC (10-100nm; <100,000 pcm ³)	Median: 19,000	*LTO* (landing, takeoffs, and sum of the two)
Hudda et al. 2020	Logan International Airport, Boston	Continuously for 1 month	CPC (10-100nm; <100,000 pcm ³)	Median; 17,000	Residence near the Logan International Airport, Boston; continuously for 1 month
Klapmeyer & Marr 2012	Roanoke Regional Airport, Virginia	24 days	CPC (10-100nm; <100,000 pcm ³)	Comparable metric not reported	Adjacent to the airfield and passenger terminal at the Roanoke Regional Airport in Virginia
Lenssen et al. 2024	3 schools; North and South of Schiphol Airport	2017–2018	GRIMM SMPS model 5420	Mean: 8,425	Hourly concentrations of various size fractions of PNC and black carbon (BC) were measured at three school yards
Pirhadi et al. 2020	Amsterdam Schiphol	32 sampling days over a 6-month period	CPC (10-100nm; <100,000 pcm ³)	Mean: 35,308	Adjacent to Schiphol airport
Westerdahl et al., 2008	Los Angeles International Airport (LAX)	Spring of 2003	CPC (10-100nm; <100,000 pcm ³)	Mean: 50,000	Mixed-use (including residential) neighbourhood adjacent to LAX during the spring of 2003
Zhu et al. 2011	Los Angeles International Airport (LAX)	Continuously on three time periods: 2005-2006: September, February, March	CPC (10-100nm; <100,000 pcm ³)	Median: ~20,000	At LAX and a background reference site

Note: Commonly used instruments 'Condensation Particle Counters (TSI 3007)' is abbreviated with 'CPC'.

The studies presented in Table 5 were conducted with different designs to the present study in Copenhagen. Due to high spatial and temporal variability within and across cities, besides different study designs, measured PNC will depend highly on factors such as the time of the day and year, the route, proximity to heavy traffic, the share of heavy diesel vehicles in proximity, and meteorology. Additionally, different instruments for measuring UFP may perform differently. A comparison of UFP concentrations measured in different studies can therefore only be made with caution.

Table 6. Overview of studies on mean UFP exposure concentrations while cycling

Authors, year	Study area	Total # of trips	Instrument, particle size range	Mean PNC (pt/cm ³)	Type of exposure
Bergmann et al. 2022	Copenhagen, Denmark	61	DiSCmini (10-300nm)	18,556 18,882 17,569	Morning rush-hour Late morning Afternoon rush-hour
Bergmann et al. 2021	Copenhagen, Denmark	43	DiSCmini (10-300nm)	11,963	Afternoon rush-hour
Yang et al. 2021	Beijing, China	10	DiSCmini (10-300nm)	28,277	Peak, Off-peak (not reported separately)
Luengo-Oroz and Reis 2019	Edinburgh, UK	54	DiSCmini (10-300nm)	19,310 9,824 7,990	High-traffic Medium-traffic Low-traffic
Qiu et al. 2019	Xi'an, China	29	P-trak (20-1000nm)	18,172	Cycling, two commute routes
Cole et al. 2018	Vancouver, Canada	76	P-trak (20-1000nm)	16,226 9,367	Downtown Residential
Hofman et al. 2018	Antwerp, Belgium	80	P-trak (20-1000nm)	16,463 9,986	Morning rush-hour Afternoon rush-hour
Okokon et al. 2017	Rotterdam, Netherlands	84	P-trak (20-1000nm)	20,000	Cycling on commuting route
Pattinson et al. 2017	Christchurch, New Zealand	15	CPC (10-100nm)	42,480 28,765 24,977	Road Sidewalk Path
Hankey and Marshall 2015	Minneapolis, USA	42	CPC (10-100nm)	35,003 18,401	Mornings Afternoons
Peters et al. 2014	Antwerp, Belgium	354	P-trak (20-1000nm)	32,310	Cycling, two commute routes
Hatzopoulou et al. 2013	Montreal, Canada	64	CPC (10-100nm)	24,800 21,800	Mornings Afternoons
Jarjour et al. 2013	Berkeley, USA	30	CPC (10-100nm)	(UFPM/cm ³) 18,545 14,311	High-traffic Low-traffic
Kingham et al. 2013	Christchurch, New Zealand	78	CPC (10-100nm)	(Median) 31,414 16,641	On-road Off-road
Ragetti et al. 2013	Basel, Switzerland	96	DiSCmini (10-300nm)	34,025 18,156	High-traffic Low traffic
Cole-Hunter et al. 2012	Brisbane, Australia	24	Aerasense NanoTracer (10-300nm)	15,600 30,600	Low traffic proximity High traffic proximity
De Nazelle et al. 2012	Barcelona, Spain	54	CPC (10-100nm)	75,300	Two commuting routes, between 7am and 1pm
Strak et al. 2010	Utrecht, Netherlands	80	CPC (10-100nm)	44,090 27,813	High-traffic Low-traffic

Zuurbier et al. 2010	Arnhem, Netherlands	30	CPC (10-100nm)	48,939 39,576	High-traffic Low-traffic
Berghmans et al. 2009	Mol, Belgium	8	P-trak (20-1000nm)	21,226	Cycling on a fixed route, different times
Boogaard et al. 2009	11 Dutch cities	120	CPC (10-100nm)	24,329	Cycling on 12 routes in 11 cities
Thai et al. 2008	Vancouver, Canada	14	P-trak (20-1000nm)	33,899	Cycling on a fixed route during morning rush-hour
Vinzents et al. 2005	Copenhagen, Denmark	75	CPC (10-100nm)	32,400 pt/mL	Cycling on a fixed route during rush-hour

Note: Commonly used instruments ‘P-trak Ultrafine Particle Counter’ and ‘Condensation Particle Counters (TSI 3007)’ are abbreviated with ‘P-Trak’ and ‘CPC’, respectively.

The studies presented in Table 6 were conducted with somewhat similar designs to the present study in Copenhagen. However, again, due to high spatial and temporal variability within and across cities, measured PNC will depend highly on factors such as the time of the day and year, the route, proximity to heavy traffic, the share of heavy diesel vehicles in proximity, and meteorology. Additionally, different instruments for measuring UFP may perform differently. A comparison of UFP concentrations measured in different studies can therefore only be made with caution.

Three comparable studies were identified that used a ‘DiSCmini’, as the current study did, and were done in the European cities, Basel and Edinburgh, and in Chinese city, Beijing. While cycling on a route in Basel at different times of the day, mean UFP concentrations of 22,660 pt/cm³ have been measured (Ragettli et al., 2013). In Edinburgh, cycling was done in high-, medium- and low-traffic contexts and mean PNC was 19,310, 9,824 and 7,990 pt/cm³, respectively (Luengo-Oroz and Reis, 2019). In Beijing, cycling was done on only one route but across peak and off-peak times, although data from these times (due to limited number of trips) were combined to give the average PNC level of 28,277 pt/cm³ (Yang et al., 2021). Thus, our previous study finding of PNC around 18,000 pt/cm³, which can be considered a high-traffic setting, are comparable, and somewhat lower than those found in Basel, Edinburgh, and Beijing; the current study’s PNC of around 10,000 pt/cm³ are higher than those seen in Edinburgh. In Antwerp, Belgium, PNC was measured during morning and afternoon rush-hours, using a ‘P-trak Ultrafine Particle Counter’, which measures particles in a wider size range of 20-1000 nm (compared to DiSCmini of 10-300nm). During morning and afternoon rush-hour, mean PNC was 16,463 and 9,986 pt/cm³, respectively (Hofman et al., 2018). Another study in Vancouver found concentrations of 16,226 and 9,367 pt/cm³ on a downtown and a residential route, respectively, using the P-trak (Cole et al., 2018). The concentrations of approximately 10,000 pt/cm³ that were measured during morning rush-hour and late periods in the current study are therefore within the range of these previous studies. Several other studies, for example in Barcelona (de Nazelle et al., 2012), Antwerp (Peters et al., 2014), Arnhem (Zuurbier et al., 2010), Utrecht (Strak et al., 2010) and a previous study in Copenhagen in 2005 (Vinzents et al., 2005) found considerably higher PNC, ranging between ~28,000 pt/cm³ on a low-traffic route in Arnhem and ~75,000 pt/cm³ in central Barcelona. These differences in UFP

concentrations may be related to different study designs or, especially in the case of the study in Copenhagen, the year of the study. Concentrations of UFP measured at different locations in Copenhagen have been reduced substantially since the year 2001. Changes in regulation and/or technology (e.g., engine emission standards) could explain a reduction in emissions without a reduction in traffic concentrations. Other changes include societal demands, such as home-delivered food within a ‘gig’ economy (e.g., app-based services such as ‘Wolt’). Future work may investigate the contribution of moped emissions to UFP concentrations on bicycle paths (used by home-delivery moped operators), which have been seen in Dutch cities to contribute up to 20% of total UFP concentrations there (Zuurbier et al., 2019).

In our previous study similar to the current study, when two new municipal UFP measurement stations were operating at Søtorvet and Krügersgade (from September 25th, 2020), we found a correlation of 80,5% (Spearman correlation-test, $p < 0.0001$) for hourly PNC between the stations and DiSCmini (when co-located). Daily means were even more closely correlated with 96.7% agreement (Spearman $p < 0.0001$). This is in line with the results in our current study in which by using 5 minutes averages of PNC in two 24-hour co-locations, we found a 93% and 95% agreement (Spearman correlation test, $p < 2.2e^{-16}$).

7. Potential health impacts of observed UFP concentrations

Airport-related UFP raises health concerns for airport workers and residents in airport vicinity, but the available evidence is still scarce, as described below. Studies have shown that short-term exposure to airport-related UFP can have adverse effects on biomarkers related to cardiovascular and respiratory health, such as lung and heart function, and changes in cellular pathway activity (Habre et al., 2018a; Lammers et al., 2020a; Selley et al., 2021a). These effects were found in healthy adults but are likely stronger among people with pre-existing diseases. Moreover, children living close to airports experienced more respiratory complaints on days with high exposures (Lenssen et al., 2024b). Long-term studies of cohorts linked to address-level airport-related UFP exposure are very few, but studies found possible associations with cardiovascular diseases, respiratory diseases among people with pre-existing conditions (Janssen et al., 2022a), malignant brain cancer (Wu et al., 2021), autism spectrum disorder (Carter et al., 2023a) and perinatal health with only preterm birth found in more than one long-term study (Wing et al., 2020a).

7.1. Short-term health effects of air quality near airports

Short-term studies evaluate whether the exposure to airport-related UFP can trigger health effects or lead to changes in biomarkers of cardiovascular or respiratory health over a course of hours or days; however, this response is not necessarily different from that elicited by road-traffic-related UFP (Janssen et al., 2019). Previously, several studies have conducted quasi-experimental studies with healthy or asthmatic volunteers walking (Habre et al., 2018b) or cycling (Lammers et al., 2020b; Selley et al., 2021b) in both clean and airport air, taking repeated measurements of biomarkers.

Adjacent to Los Angeles International Airport, 22 asthmatic adults walked on two occasions for two hours each in public parks inside and outside of a zone impacted by airport-related UFP. Repeated measurements of cardiopulmonary markers showed associations between airport-related UFP and increased systemic inflammation (Habre et al., 2018b).

Adjacent to Schiphol Airport close to Amsterdam, 21 healthy adults bicycled for five hours each both in airport-UFP-affected ambient air and clean air (Lammers et al., 2020b). Repeated measurements of health markers showed associations between airport-related UFP and decreased lung function (mainly FVC), and worsened cardiovascular (prolonged corrected QT interval) and metabolic (changed urinary metabolome, indicating a heightened antioxidant response and altered nitric oxide synthesis) markers of health (Selley et al., 2021b). More recently, in the same region, a study found that emissions from airports (aviation exhaust) was related to an increase in respiratory symptoms, although not lung function, among children (Lenssen et al., 2024a).

7.2. Long-term health effects of air quality near airports

Population-based cohort studies of long-term exposure to airport-related UFP and associated health effects are scarce. The only available studies were conducted around Schiphol Airport (Janssen et al., 2022b), LAX (Wing et al., 2020b; Wu et al., 2021), and in all of California (Carter et al., 2023b).

The Dutch studies were summarized in a report including findings on mortality, use of medication, perinatal health and self-reported health as outcomes. Airport-related UFP in 2003-2019 was modelled for a large study population (number differing by sub-study, e.g. ~1.3 million in mortality study) living in an area of 50x55 km around Schiphol Airport. Summarizing the different sub-studies, the authors conclude that there was no indication for associations between long-term exposure to airport-related UFP and general health. For respiratory diseases, adverse effects were only seen for people with pre-existing conditions, while there was suggestive evidence for an association between long-term exposure to airport-related UFP and cardiovascular diseases (i.e., arrhythmia mortality, heart disease medication use, and self-reported heart disease and stroke). Further suggestive evidence was found for an association between long-term exposure to airport-related UFP and perinatal health (i.e. preterm birth, small for gestational age, and congenital anomalies). Evidence regarding the nervous and metabolic system was too inadequate for drawing conclusions (Janssen et al., 2022b).

The studies around LAX focused on malignant brain cancer and meningioma (Wu et al., 2021), and preterm birth (Wing et al., 2020b). The former study modelled airport-related UFP for 75,936 residents in an area of 53x43 km around LAX from date of cohort entry (1993–1996) through the end of 2013. An IQR (6,700 pt/cm³) increase in long-term exposure to airport-related UFP was associated with a HR of 1.12 (95% CI: 0.98, 1.27) with the incidence of malignant brain cancer, after adjusting for sex, race/ethnicity, education, and neighbourhood socioeconomic status. No associations were found with meningioma. In the latter study, airport-related UFP exposure was modelled for 174,186 women who gave birth between 2008 and 2016, living within 15 km from LAX. Using birth records and adjusting for maternal demographic characteristics, exposure to traffic-related air pollution, and airport-related noise, the authors found a significant association between *in utero* exposure to airport-related UFP and preterm birth (OR: 1.04 [95% CI: 1.02, 1.06] per 9,200 pt/cm³).

One study used modelled airport-related UFP exposure for the whole state of California and included 370,723 singletons born in selected hospitals in California between 2001 and 2014. Airport-related UFP exposure was assigned to the mothers' address during pregnancy, and children were followed up for the first five years of their life. An IQR (0.02 µg/m³) increase in *in utero* airport-related PM_{0.1} exposure was associated with autism spectrum disorder diagnosis with a HR of 1.02 (95% CI: 1.01, 1.03), adjusting for birth year, medical centre, maternal age, maternal ethnicity, maternal education, parity, history of comorbidity, income at age one, season of conception, pre-pregnancy diabetes mellitus, pre-pregnancy obesity, and child's sex (Carter et al., 2023b).

8. Conclusion

In our study measuring UFP concentrations while bicycling through a residential area of the Amager neighbourhood, Denmark, we found overall low UFP concentrations, as an average of 7,620 pt/cm³, consistent with its residential location. We also found that UFP concentrations were highest on days with wind from the south or south-east, as an average of 13,067 and 11,237 pt/cm³, respectively, and lowest with northwest wind, as an average of 3,479 pt/cm³. In addition, on days with south wind, we observed a gradient of increasing UFP concentrations from north to south (~12,000 to ~15,000 pt/cm³). This suggests the likely influence of the airport as a contributor to UFP levels, as the airport is located south-east of the bicycling route. This finding is in line with other studies, which have seen elevated UFP concentrations as far as 18 km away from airports, mostly related to the departure and arrival of airplanes. Our measurements also confirmed the typically observed concentration peaks close to busy roads, traffic congestion or traffic lights (~10,000 to ~12,000 pt/cm³), confirming road traffic as another contributor to UFP levels. These 'hotspot' (peak UFP) areas were still observed, but increased in magnitude, on days with southerly wind (~15,000 pt/cm³).

Our study raises concerns of higher UFP concentrations in Eastern Amager neighbourhood on days with south or south-east wind, indicative of a contribution by airport activity. While we did not measure health effects in our study, previous studies suggest that increased UFP exposure during bicycling may be associated with biomarkers related to cardiovascular and respiratory diseases. The available evidence on morbidity and mortality associated with short- or long-term UFP exposure in general is still very scarce, as UFP are not regulated and not included in routine monitoring of air pollution, and more research is needed. In general, cyclists can effectively reduce their exposure to UFP by avoiding major traffic roads that experience congestion due to traffic volumes or traffic control measures (e.g., traffic lights at busy intersections). Thus, to reduce traffic-related UFP exposure, it is commonly advised to choose bicycling/walking paths further away from roads, such as in green or blue areas (e.g., Amager Strandpark). However, our study points out that Copenhagen International airport activities can contribute to UFP levels in residential neighbourhoods kilometres away from the airport itself, though only on days with favourable wind conditions. It is still not clear how these increases in UFPs levels in Amager, only on the days with southerly and south-easterly wind, affect health, both in the short and long term, as research is still very limited on this topic.

References

- Alzahrani, S., Kılıç, D., Flynn, M., Williams, P.I., Allan, J., 2024. International airport emissions and their impact on local air quality: chemical speciation of ambient aerosols at Madrid–Barajas Airport during the AVIATOR campaign. *Atmospheric Chem. Phys.* 24, 9045–9058. <https://doi.org/10.5194/acp-24-9045-2024>
- Austin, E., Xiang, J., Gould, T.R., Shirai, J.H., Yun, S., Yost, M.G., Larson, T.V., Seto, E., 2021. Distinct Ultrafine Particle Profiles Associated with Aircraft and Roadway Traffic. *Environ. Sci. Technol.* 55, 2847–2858. <https://doi.org/10.1021/acs.est.0c05933>
- Bendtsen, K.M., Bengtson, E., Saber, A.T., Vogel, U., 2021. A review of health effects associated with exposure to jet engine emissions in and around airports. *Environ. Health Glob. Access Sci. Source* 20, 10. <https://doi.org/10.1186/s12940-020-00690-y>
- Berghmans, P., Bleux, N., Panis, L.I., Mishra, V.K., Torfs, R., Van Poppel, M., 2009. Exposure assessment of a cyclist to PM10 and ultrafine particles. *Sci. Total Environ.* 407, 1286–1298. <https://doi.org/10.1016/j.scitotenv.2008.10.041>
- Bergmann, M.L., Andersen, Z.J., Amini, H., Ellermann, T., Hertel, O., Lim, Y.H., Loft, S., Mehta, A., Westendorp, R.G., Cole-Hunter, T., 2021. Exposure to ultrafine particles while walking or bicycling during COVID-19 closures: A repeated measures study in Copenhagen, Denmark. *Sci. Total Environ.* 791, 148301. <https://doi.org/10.1016/j.scitotenv.2021.148301>
- Bergmann, M.L., Andersen, Z.J., Amini, H., Khan, J., Lim, Y.H., Loft, S., Mehta, A., Westendorp, R.G., Cole-Hunter, T., 2022. Ultrafine particle exposure for bicycle commutes in rush and non-rush hour traffic: A repeated measures study in Copenhagen, Denmark. *Environ. Pollut.* 294, 118631. <https://doi.org/10.1016/j.envpol.2021.118631>
- Boogaard, H., Borgman, F., Kamminga, J., Hoek, G., 2009. Exposure to ultrafine and fine particles and noise during cycling and driving in 11 Dutch cities. *Atmos. Environ.* 43, 4234–4242. <https://doi.org/10.1016/j.atmosenv.2009.05.035>
- Cappelen, J., 2021. Denmark – DMI Historical Climate Data Collection 1768-2020.
- Carter, S.A., Rahman, M.M., Lin, J.C., Chow, T., Yu, X., Martinez, M.P., Levitt, P., Chen, Z., Chen, J.-C., Eckel, S.P., Schwartz, J., Lurmann, F.W., Kleeman, M.J., McConnell, R., Xiang, A.H., 2023a. Maternal exposure to aircraft emitted ultrafine particles during pregnancy and likelihood of ASD in children. *Environ. Int.* 178, 108061. <https://doi.org/10.1016/j.envint.2023.108061>
- Carter, S.A., Rahman, M.M., Lin, J.C., Chow, T., Yu, X., Martinez, M.P., Levitt, P., Chen, Z., Chen, J.-C., Eckel, S.P., Schwartz, J., Lurmann, F.W., Kleeman, M.J., McConnell, R., Xiang, A.H., 2023b. Maternal exposure to aircraft emitted ultrafine particles during pregnancy and likelihood of ASD in children. *Environ. Int.* 178, 108061. <https://doi.org/10.1016/j.envint.2023.108061>
- Choi, W., Hu, S., He, M., Kozawa, K., Mara, S., Winer, A.M., Paulson, S.E., 2013. Neighborhood-scale air quality impacts of emissions from motor vehicles and aircraft. *Atmos. Environ.* 80, 310–321. <https://doi.org/10.1016/j.atmosenv.2013.07.043>
- Chung, C.S., Lane, K.J., Black-Ingersoll, F., Kolaczyk, E., Schollaert, C., Li, S., Simon, M.C., Levy, J.I., 2023. Assessing the impact of aircraft arrival on ambient ultrafine particle number concentrations in near-airport communities in Boston, Massachusetts. *Environ. Res.* 225, 115584. <https://doi.org/10.1016/j.envres.2023.115584>
- Cole, C.A., Carlsten, C., Koehle, M., Brauer, M., 2018. Particulate matter exposure and health impacts of urban cyclists: a randomized crossover study. *Environ. Health* 17, 78. <https://doi.org/10.1186/s12940-018-0424-8>
- Cole-Hunter, T., Morawska, L., Stewart, I., Jayaratne, R., Solomon, C., 2012. Inhaled particle counts on bicycle commute routes of low and high proximity to motorised traffic. *Atmos. Environ.* 61, 197–203. <https://doi.org/10.1016/j.atmosenv.2012.06.041>
- Copenhagen Airport Guide, 2024. Statistics for Copenhagen Airport.
- Corbin, J.C., Schripp, T., Anderson, B.E., Smallwood, G.J., LeClercq, P., Crosbie, E.C., Achterberg, S., Whitefield, P.D., Miake-Lye, R.C., Yu, Z., Freedman, A., Trueblood, M., Satterfield, D., Liu, W., Oßwald, P., Robinson, C., Shook, M.A., Moore, R.H., Lobo, P., 2022. Aircraft-engine

- particulate matter emissions from conventional and sustainable aviation fuel combustion: comparison of measurement techniques for mass, number, and size. *Atmospheric Meas. Tech.* 15, 3223–3242. <https://doi.org/10.5194/amt-15-3223-2022>
- de Nazelle, A., Fruin, S., Westerdahl, D., Martinez, D., Ripoll, A., Kubesch, N., Nieuwenhuijsen, M., 2012. A travel mode comparison of commuters' exposures to air pollutants in Barcelona. *Atmos. Environ.* 59, 151–159. <https://doi.org/10.1016/j.atmosenv.2012.05.013>
- Dröge, J., Klingelhöfer, D., Braun, M., Groneberg, D.A., 2024. Influence of a large commercial airport on the ultrafine particle number concentration in a distant residential area under different wind conditions and the impact of the COVID-19 pandemic. *Environ. Pollut.* 345, 123390. <https://doi.org/10.1016/j.envpol.2024.123390>
- Ellermann, T., Massling, A., Løfstrøm, P., Winther, M., Nøjgaard, J., Ketzel, M., 2012. Assessment of the air quality at the apron of Copenhagen Airport Kastrup in relation to the working environment. Aarhus University, DCE - Danish Centre for Environment and Energy 51.
- Force Technology, F., 2024. Overvågning af luftkvalitet i Københavns Kommune.
- Fritz, S., Grusdat, F., Sharkey, R., Schneider, C., 2022. Impact of airport operations and road traffic on the particle number concentration in the vicinity of a suburban airport. *Front. Environ. Sci.* 10, 887493. <https://doi.org/10.3389/fenvs.2022.887493>
- Gerling, L., Weber, S., 2023. Mobile measurements of atmospheric pollutant concentrations in the pollutant plume of BER airport. *Atmos. Environ.* 304, 119770. <https://doi.org/10.1016/j.atmosenv.2023.119770>
- Habre, R., Zhou, H., Eckel, S.P., Enebish, T., Fruin, S., Bastain, T., Rappaport, E., Gilliland, F., 2018a. Short-term effects of airport-associated ultrafine particle exposure on lung function and inflammation in adults with asthma. *Environ. Int.* 118, 48–59. <https://doi.org/10.1016/j.envint.2018.05.031>
- Habre, R., Zhou, H., Eckel, S.P., Enebish, T., Fruin, S., Bastain, T., Rappaport, E., Gilliland, F., 2018b. Short-term effects of airport-associated ultrafine particle exposure on lung function and inflammation in adults with asthma. *Environ. Int.* 118, 48–59. <https://doi.org/10.1016/j.envint.2018.05.031>
- Hankey, S., Marshall, J.D., 2015. On-bicycle exposure to particulate air pollution: Particle number, black carbon, PM 2.5, and particle size. *Atmos. Environ.* 122, 65–73. <https://doi.org/10.1016/j.atmosenv.2015.09.025>
- Hatzopoulou, M., Weichenthal, S., Dugum, H., Pickett, G., Miranda-Moreno, L., Kulka, R., Andersen, R., Goldberg, M., 2013. The impact of traffic volume, composition, and road geometry on personal air pollution exposures among cyclists in Montreal, Canada. *J. Expo. Sci. Environ. Epidemiol.* 23, 46–51. <https://doi.org/10.1038/jes.2012.85>
- Health Effects Institute, 2024. State of Global Air 2024. Special Report. Boston, MA.
- Hofman, J., Samson, R., Joosen, S., Blust, R., Lenaerts, S., 2018. Cyclist exposure to black carbon, ultrafine particles and heavy metals: An experimental study along two commuting routes near Antwerp, Belgium. *Environ. Res.* 164, 530–538. <https://doi.org/10.1016/j.envres.2018.03.004>
- Hsu, H.-H., Adamkiewicz, G., Houseman, E.A., Spengler, J.D., Levy, J.I., 2014. Using mobile monitoring to characterize roadway and aircraft contributions to ultrafine particle concentrations near a mid-sized airport. *Atmos. Environ.* 89, 688–695. <https://doi.org/10.1016/j.atmosenv.2014.02.023>
- Hsu, H.-H., Adamkiewicz, G., Houseman, E.A., Zarubiak, D., Spengler, J.D., Levy, J.I., 2013. Contributions of aircraft arrivals and departures to ultrafine particle counts near Los Angeles International Airport. *Sci. Total Environ.* 444, 347–355. <https://doi.org/10.1016/j.scitotenv.2012.12.010>
- Hu, S., Fruin, S., Kozawa, K., Mara, S., Winer, A.M., Paulson, S.E., 2009. Aircraft Emission Impacts in a Neighborhood Adjacent to a General Aviation Airport in Southern California. *Environ. Sci. Technol.* 43, 8039–8045. <https://doi.org/10.1021/es900975f>

- Hudda, N., Durant, L.W., Fruin, S.A., Durant, J.L., 2020. Impacts of Aviation Emissions on Near-Airport Residential Air Quality. *Environ. Sci. Technol.* 54, 8580–8588. <https://doi.org/10.1021/acs.est.0c01859>
- Hudda, N., Fruin, S.A., 2016. International Airport Impacts to Air Quality: Size and Related Properties of Large Increases in Ultrafine Particle Number Concentrations. *Environ. Sci. Technol.* 50, 3362–3370. <https://doi.org/10.1021/acs.est.5b05313>
- Hudda, N., Gould, T., Hartin, K., Larson, T.V., Fruin, S.A., 2014. Emissions from an international airport increase particle number concentrations 4-fold at 10 km downwind. *Environ. Sci. Technol.* 48, 6628–6635. <https://doi.org/10.1021/es5001566>
- Hudda, N., Simon, M.C., Zamore, W., Brugge, D., Durant, J.L., 2016. Aviation Emissions Impact Ambient Ultrafine Particle Concentrations in the Greater Boston Area. *Environ. Sci. Technol.* 50, 8514–8521. <https://doi.org/10.1021/acs.est.6b01815>
- Hudda, N., Simon, M.C., Zamore, W., Durant, J.L., 2018. Aviation-Related Impacts on Ultrafine Particle Number Concentrations Outside and Inside Residences near an Airport. *Environ. Sci. Technol.* 52, 1765–1772. <https://doi.org/10.1021/acs.est.7b05593>
- Janssen, N., Hoekstra, J., Houthuijs, D., Jacobs, J., Nicolaie, A., Strak, M., 2022a. Effects of long-term exposure to ultrafine particles from aviation around Schiphol Airport. Rijksinstituut voor Volksgezondheid en Milieu RIVM. <https://doi.org/10.21945/RIVM-2022-0068>
- Janssen, N., Hoekstra, J., Houthuijs, D., Jacobs, J., Nicolaie, A., Strak, M., 2022b. Effects of long-term exposure to ultrafine particles from aviation around Schiphol Airport. Rijksinstituut voor Volksgezondheid en Milieu RIVM. <https://doi.org/10.21945/RIVM-2022-0068>
- Janssen, N.A.H., Lammer, M., Maitland-Van De Zee, A.H., Van De Zee, S., Keuken, R., Blom, M., Van Den Bulk, P., Van Dinther, D., Hoek, G., Kamstra, K., Meliefste, K., Oldenwenning, M., Boere, A.J.F., Cassee, F.R., Fischer, P.H., Gerlofs-Nijland, M.E., Houthuijs, D., 2019. Onderzoek naar de gezondheidseffecten van kortdurende blootstelling aan ultrafijn stof rond Schiphol. <https://doi.org/10.21945/RIVM-2019-0084>
- Kaur, S., Nieuwenhuijsen, M., Colvile, R., 2005. Personal exposure of street canyon intersection users to PM_{2.5}, ultrafine particle counts and carbon monoxide in Central London, UK. *Atmos. Environ.* 39, 3629–3641. <https://doi.org/10.1016/j.atmosenv.2005.02.046>
- Kerckhoffs, J., Khan, J., Hoek, G., Yuan, Z., Hertel, O., Ketznel, M., Jensen, S.S., Al Hasan, F., Meliefste, K., Vermeulen, R., 2022. Hyperlocal variation of nitrogen dioxide, black carbon, and ultrafine particles measured with Google Street View cars in Amsterdam and Copenhagen. *Environ. Int.* 170, 107575. <https://doi.org/10.1016/j.envint.2022.107575>
- Keuken, M.P., Moerman, M., Zandveld, P., Henzing, J.S., Hoek, G., 2015. Total and size-resolved particle number and black carbon concentrations in urban areas near Schiphol airport (the Netherlands). *Atmos. Environ.* 104, 132–142. <https://doi.org/10.1016/j.atmosenv.2015.01.015>
- Klapmeyer, M.E., Marr, L.C., 2012. CO₂, NO_x, and Particle Emissions from Aircraft and Support Activities at a Regional Airport. *Environ. Sci. Technol.* 46, 10974–10981. <https://doi.org/10.1021/es302346x>
- Lammers, A., Janssen, N. a. H., Boere, A.J.F., Berger, M., Longo, C., Vijverberg, S.J.H., Neerincx, A.H., Maitland-van der Zee, A.H., Cassee, F.R., 2020a. Effects of short-term exposures to ultrafine particles near an airport in healthy subjects. *Environ. Int.* 141, 105779. <https://doi.org/10.1016/j.envint.2020.105779>
- Lammers, A., Janssen, N. a. H., Boere, A.J.F., Berger, M., Longo, C., Vijverberg, S.J.H., Neerincx, A.H., Maitland-van der Zee, A.H., Cassee, F.R., 2020b. Effects of short-term exposures to ultrafine particles near an airport in healthy subjects. *Environ. Int.* 141, 105779. <https://doi.org/10.1016/j.envint.2020.105779>
- Lenssen, E.S., Janssen, N.A.H., Oldenwenning, M., Meliefste, K., de Jonge, D., Kamstra, R.J.M., van Dinther, D., van der Zee, S., Keuken, R.H., Hoek, G., 2024a. Beyond the Runway: Respiratory

- health effects of ultrafine particles from aviation in children. *Environ. Int.* 188, 108759. <https://doi.org/10.1016/j.envint.2024.108759>
- Lenzen, E.S., Janssen, N.A.H., Oldenwening, M., Meliefste, K., de Jonge, D., Kamstra, R.J.M., van Dinther, D., van der Zee, S., Keuken, R.H., Hoek, G., 2024b. Beyond the Runway: Respiratory health effects of ultrafine particles from aviation in children. *Environ. Int.* 188, 108759. <https://doi.org/10.1016/j.envint.2024.108759>
- Luengo-Oroz, J., Reis, S., 2019. Assessment of cyclists' exposure to ultrafine particles along alternative commuting routes in Edinburgh. *Atmospheric Pollut. Res.* 10, 1148–1158. <https://doi.org/10.1016/j.apr.2019.01.020>
- Masiol, M., Vu, T.V., Beddows, D.C.S., Harrison, R.M., 2016. Source apportionment of wide range particle size spectra and black carbon collected at the airport of Venice (Italy). *Atmos. Environ.* 139, 56–74. <https://doi.org/10.1016/j.atmosenv.2016.05.018>
- Møller, K.L., Thygesen, L.C., Schipperijn, J., Loft, S., Bonde, J.P., Mikkelsen, S., Brauer, C., 2014. Occupational Exposure to Ultrafine Particles among Airport Employees - Combining Personal Monitoring and Global Positioning System. *PLOS ONE* 9, e106671. <https://doi.org/10.1371/journal.pone.0106671>
- Morawska, L., Wierzbicka, A., Cyrus, J., Schnelle, J., Kowalski, M., Riediker, M., Birmili, W., Querol, X., Cassee, F.R., Yildirim, A.Ö., Yu, I.J., Øvreivik, J., Sørig, K., Loft, S., Schmid, O., Stöger, T., 2019. Ambient ultrafine particles: evidence for policy makers.
- Ohlwein, S., Kappeler, R., Kutlar Joss, M., Künzli, N., Hoffmann, B., 2019. Health effects of ultrafine particles: a systematic literature review update of epidemiological evidence. *Int. J. Public Health* 64, 547–559. <https://doi.org/10.1007/s00038-019-01202-7>
- Pattinson, W., Kingham, S., Longley, I., Salmond, J., 2017. Potential pollution exposure reductions from small-distance bicycle lane separations. *J. Transp. Health* 4, 40–52. <https://doi.org/10.1016/j.jth.2016.10.002>
- Peters, J., Van den Bossche, J., Reggente, M., Van Poppel, M., De Baets, B., Theunis, J., 2014. Cyclist exposure to UFP and BC on urban routes in Antwerp, Belgium. *Atmos. Environ.* 92, 31–43. <https://doi.org/10.1016/j.atmosenv.2014.03.039>
- Pirhadi, M., Mousavi, A., Sowlat, M.H., Janssen, N.A.H., Cassee, F.R., Sioutas, C., 2020. Relative contributions of a major international airport activities and other urban sources to the particle number concentrations (PNCs) at a nearby monitoring site. *Environ. Pollut. Barking Essex* 1987 260, 114027. <https://doi.org/10.1016/j.envpol.2020.114027>
- Qiu, Z., Wang, W., Zheng, J., Lv, H., 2019. Exposure assessment of cyclists to UFP and PM on urban routes in Xi'an, China. *Environ. Pollut.* 250, 241–250. <https://doi.org/10.1016/j.envpol.2019.03.129>
- Ragettli, M.S., Corradi, E., Braun-Fahrländer, C., Schindler, C., de Nazelle, A., Jerrett, M., Ducret-Stich, R.E., Künzli, N., Phuleria, H.C., 2013. Commuter exposure to ultrafine particles in different urban locations, transportation modes and routes. *Atmos. Environ.* 77, 376–384. <https://doi.org/10.1016/j.atmosenv.2013.05.003>
- Riley, E.A., Gould, T., Hartin, K., Fruin, S.A., Simpson, C.D., Yost, M.G., Larson, T., 2016. Ultrafine particle size as a tracer for aircraft turbine emissions. *Atmos. Environ.* 139, 20–29. <https://doi.org/10.1016/j.atmosenv.2016.05.016>
- Riley, K., Cook, R., Carr, E., Manning, B., 2021. A Systematic Review of The Impact of Commercial Aircraft Activity on Air Quality Near Airports. *City Environ. Interact.* 11. <https://doi.org/10.1016/j.cacint.2021.100066>
- Selley, L., Lammers, A., Le Guennec, A., Pirhadi, M., Sioutas, C., Janssen, N., Maitland-van der Zee, A.H., Mudway, I., Cassee, F., 2021a. Alterations to the urinary metabolome following semi-controlled short exposures to ultrafine particles at a major airport. *Int. J. Hyg. Environ. Health* 237, 113803. <https://doi.org/10.1016/j.ijheh.2021.113803>
- Selley, L., Lammers, A., Le Guennec, A., Pirhadi, M., Sioutas, C., Janssen, N., Maitland-van der Zee, A.H., Mudway, I., Cassee, F., 2021b. Alterations to the urinary metabolome following semi-

- controlled short exposures to ultrafine particles at a major airport. *Int. J. Hyg. Environ. Health* 237, 113803. <https://doi.org/10.1016/j.ijheh.2021.113803>
- Shirmohammadi, F., Sowlat, M.H., Hasheminassab, S., Saffari, A., Ban-Weiss, G., Sioutas, C., 2017. Emission rates of particle number, mass and black carbon by the Los Angeles International Airport (LAX) and its impact on air quality in Los Angeles. *Atmos. Environ.* 151, 82–93. <https://doi.org/10.1016/j.atmosenv.2016.12.005>
- Stacey, B., Harrison, R.M., Pope, F., 2020. Evaluation of ultrafine particle concentrations and size distributions at London Heathrow Airport. *Atmos. Environ.* 222, 117148. <https://doi.org/10.1016/j.atmosenv.2019.117148>
- Strak, M., Boogaard, H., Meliefste, K., Oldenwening, M., Zuurbier, M., Brunekreef, B., Hoek, G., 2010. Respiratory health effects of ultrafine and fine particle exposure in cyclists. *Occup. Environ. Med.* 67, 118–124. <https://doi.org/10.1136/oem.2009.046847>
- Tainio, M., De Nazelle, A.J., Götschi, T., Kahlmeier, S., Rojas-Rueda, D., Nieuwenhuijsen, M.J., De Sá, T.H., Kelly, P., Woodcock, J., 2016. Can air pollution negate the health benefits of cycling and walking? *Prev. Med.* 87, 233–236. <https://doi.org/10.1016/j.ypmed.2016.02.002>
- Thai, A., McKendry, I., Brauer, M., 2008. Particulate matter exposure along designated bicycle routes in Vancouver, British Columbia. *Sci. Total Environ.* 405, 26–35. <https://doi.org/10.1016/j.scitotenv.2008.06.035>
- Tremper, A.H., Jephcote, C., Gulliver, J., Hibbs, L., Green, D.C., Font, A., Priestman, M., Hansell, A.L., Fuller, G.W., 2022. Sources of particle number concentration and noise near London Gatwick Airport. *Environ. Int.* 161, 107092. <https://doi.org/10.1016/j.envint.2022.107092>
- Vinzents, P.S., Møller, P., Sørensen, M., Knudsen, L.E., Hertel, O., Jensen, F.P., Schibye, B., Loft, S., 2005. Personal Exposure to Ultrafine Particles and Oxidative DNA Damage. *Environ. Health Perspect.* 113, 1485–1490. <https://doi.org/10.1289/ehp.7562>
- Wang, Q., Wang, P., Chen, H., Ma, J., Jia, Y., Wang, C., Qiao, L., Fu, Q., Mellouki, A., Li, L., 2024. Unraveling Contributions from Combustion, Secondary, Traffic, and Dust Sources through Particle Mass Size Distribution Measurement. *Aerosol Air Qual. Res.* 24, 240135. <https://doi.org/10.4209/aaqr.240135>
- Westerdahl, D., Fruin, S., Fine, P., Sioutas, C., 2008. The Los Angeles International Airport as a source of ultrafine particles and other pollutants to nearby communities. *Atmos. Environ.* 42, 3143–3155. <https://doi.org/10.1016/j.atmosenv.2007.09.006>
- WHO, 2021. WHO global air quality guidelines. Particulate matter, ozone, nitrogen dioxide, sulfur dioxide and carbon dioxide.
- Wing, S.E., Larson, T.V., Hudda, N., Boonyarattaphan, S., Fruin, S., Ritz, B., 2020a. Preterm Birth among Infants Exposed to in Utero Ultrafine Particles from Aircraft Emissions. *Environ. Health Perspect.* 128, 047002. <https://doi.org/10.1289/EHP5732>
- Wing, S.E., Larson, T.V., Hudda, N., Boonyarattaphan, S., Fruin, S., Ritz, B., 2020b. Preterm Birth among Infants Exposed to in Utero Ultrafine Particles from Aircraft Emissions. *Environ. Health Perspect.* 128, 047002. <https://doi.org/10.1289/EHP5732>
- Wu, A.H., Fruin, S., Larson, T.V., Tseng, C.-C., Wu, J., Yang, J., Jain, J., Shariff-Marco, S., Inamdar, P.P., Setiawan, V.W., Porcel, J., Stram, D.O., Le Marchand, L., Ritz, B., Cheng, I., 2021. Association between Airport-Related Ultrafine Particles and Risk of Malignant Brain Cancer: A Multiethnic Cohort Study. *Cancer Res.* 81, 4360–4369. <https://doi.org/10.1158/0008-5472.CAN-21-1138>
- Yang, Z., He, Z., Zhang, K., Zeng, L., De Nazelle, A., 2021. Investigation into Beijing commuters' exposure to ultrafine particles in four transportation modes: bus, car, bicycle and subway. *Atmos. Environ.* 266, 118734. <https://doi.org/10.1016/j.atmosenv.2021.118734>
- Yim, S.H.L., Lee, G.L., Lee, I.H., Allroggen, F., Ashok, A., Caiazzo, F., Eastham, S.D., Malina, R., Barrett, S.R.H., 2015. Global, regional and local health impacts of civil aviation emissions. *Environ. Res. Lett.* 10, 034001. <https://doi.org/10.1088/1748-9326/10/3/034001>

- Zhang, X., Karl, M., Zhang, L., Wang, J., 2020. Influence of Aviation Emission on the Particle Number Concentration near Zurich Airport. *Environ. Sci. Technol.* 54, 14161–14171. <https://doi.org/10.1021/acs.est.0c02249>
- Zhu, Y., Fanning, E., Yu, R.C., Zhang, Q., Froines, J.R., 2011. Aircraft emissions and local air quality impacts from takeoff activities at a large International Airport. *Atmos. Environ.* 45, 6526–6533. <https://doi.org/10.1016/j.atmosenv.2011.08.062>
- Zurbier, M., Hoek, G., Oldenwening, M., Lenters, V., Meliefste, K., van den Hazel, P., Brunekreef, B., 2010. Commuters' Exposure to Particulate Matter Air Pollution Is Affected by Mode of Transport, Fuel Type, and Route. *Environ. Health Perspect.* 118, 783–789. <https://doi.org/10.1289/ehp.0901622>
- Zurbier, M., Willems, J., Schaap, I., Van Der Zee, S., Hoek, G., 2019. The contribution of moped emissions to ultrafine and fine particle concentrations on bike lanes. *Sci. Total Environ.* 686, 191–198. <https://doi.org/10.1016/j.scitotenv.2019.05.409>

Appendix

Figure A1. Smoothing plots for mean hourly wind speed, ambient temperature, humidity and time trends, resulting from a GAM.

